



저작자표시-비영리-변경금지 2.0 대한민국

이용자는 아래의 조건을 따르는 경우에 한하여 자유롭게

- 이 저작물을 복제, 배포, 전송, 전시, 공연 및 방송할 수 있습니다.

다음과 같은 조건을 따라야 합니다:



저작자표시. 귀하는 원저작자를 표시하여야 합니다.



비영리. 귀하는 이 저작물을 영리 목적으로 이용할 수 없습니다.



변경금지. 귀하는 이 저작물을 개작, 변형 또는 가공할 수 없습니다.

- 귀하는, 이 저작물의 재이용이나 배포의 경우, 이 저작물에 적용된 이용허락조건을 명확하게 나타내어야 합니다.
- 저작권자로부터 별도의 허가를 받으면 이러한 조건들은 적용되지 않습니다.

저작권법에 따른 이용자의 권리는 위의 내용에 의하여 영향을 받지 않습니다.

이것은 [이용허락규약\(Legal Code\)](#)을 이해하기 쉽게 요약한 것입니다.

[Disclaimer](#)

Dissertation of Master of Engineering

A Study on the Development of
Object-oriented Route Planning
Technique for Smart Navigation based
on Risk Contours



Advisor Lee, Eun-Bang

February 2019

Maritime Safety and Environment
Department of Coast Guard Studies
Graduate School
Korea Maritime and Ocean University

Jeong, Min-Gi

Approved by the Committee of the Department of Coast
Guard Studies of Korea Maritime and Ocean University
in Fulfillment of the Requirements for the Degree of
Master's in Engineering

Dissertation Committee:

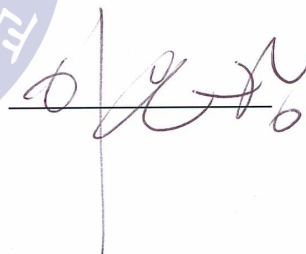
Prof. Gug, Seung-Gi, Chair



Prof. Park, Young-Soo, Reviewer



Prof. Lee, Eun-Bang, Advisor



February 2019

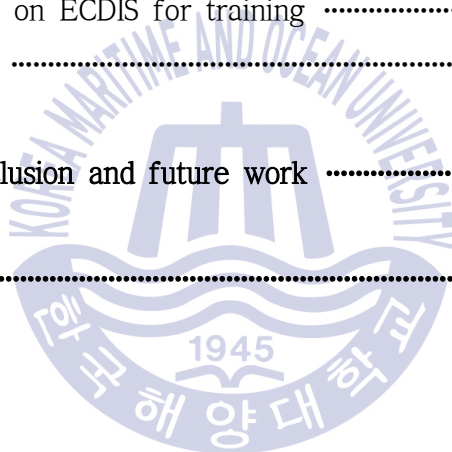
Maritime Safety and Environment Engineering
Department of Coast Guard Studies
Korea Maritime and Ocean Universities

Table of Contents

List of Tables	vi
List of Figures	v
Abstract	vi
Chapter 1. Introduction	1
1.1 Background and Purpose	1
1.2 Scope and Method	3
Chapter 2. Analysis of Related Works	7
2.1 Phase of navigation	7
2.2 Phase of route planning	9
2.3 Route planning methods	12
2.3.1 Categorization of route planning methods	12
2.3.2 Efficiency-based and economy-based route planning	14
2.3.3 Safety-based route planning	15
2.4 Navigational traffic accident and risk	17
2.4.1 Definition of navigational traffic accident	17
2.4.2 Definition of navigational traffic risk	19

Chapter 3. Risk Contour Visualization Framework	21
3.1 Formulation of Study	21
3.1.1 Experimental area (Janganseong)	21
3.1.2 Experimental ship	23
3.2 Risk Assessment Model	25
3.2.1 Data structure of risk assessment	25
3.2.2 Assessment of maritime traffic risk	27
3.2.3 Unit area for risk assessment	28
3.2.4 Filtering absolute danger	31
3.2.5 Quantification of hazard factor	33
3.2.6 Quantification of influential factor	35
3.3 Risk contour mapping	38
3.3.1 Use of contours	38
3.3.2 Concept of risk contour	38
3.3.3 Procedure of risk contour visualization	40
3.3.4 Novelty of risk contour visualization model	42
Chapter 4. Object-oriented Route Planning Technique	44
4.1 Objects of route planning	44
4.2 Assessment of objects	45
4.3 Contour-based route planning algorithm	48
4.3.1 Defining navigational direction	51
4.3.2 Route projection based on risk gradient	53
4.3.3 Route projection based on risk gradient	57
4.3.4 Object-oriented route and smart navigation	62

Chapter 5. Simulation Result and Application	63
5.1 Experimental case study of numerical simulation	63
5.1.1 Overview of numerical simulation	63
5.1.2 Results of objected-oriented routes	64
5.2 Application of object-oriented route technique	69
5.2.1 Evaluation of used routes	69
5.2.2 Analysis of navigational traffic accidents	75
5.3 Integration on ECDIS for training	86
5.4 Discussion	88
 Chapter 6. Conclusion and future work	 90
 References	 93



List of Tables

Table 1 Structured analysis of works related to route planning	13
Table 2 Elements affecting the safety of maritime traffic	28
Table 3 Elements affecting the safety of maritime traffic	36
Table 4 Result of the simulation for the object-oriented routes under the default condition	68
Table 5 Result of the simulation for the object-oriented routes under the changed condition	68
Table 6 Grounding accident of cargo ship SUN VIEW in study area	76
Table 7 Grounding accident of container ship RENA in another area	83



List of Figures

Fig. 1	Organizational flow chart of the study	6
Fig. 2	Conceptual diagram for phases of navigation	8
Fig. 3	Four phases of route planning	10
Fig. 4	Experimental area for study (Janganseong)	21
Fig. 5	Detailed description of study area on nautical chart	22
Fig. 6	Principal specification of the experimental ship	24
Fig. 7	Data structure as variables for assessment of navigational traffic risk	26
Fig. 8	Actual route plan on board modeled ships in study area	29
Fig. 9	Conceptual diagram of unit area for assessment	30
Fig. 10	Use of raw bathymetry data from Korea Hydrographic Office	32
Fig. 11	Analysis of obstacles within the unit area using clustering	33
Fig. 12	Available data from observatories for influential factor	37
Fig. 13	Examples of contours in diverse areas	39
Fig. 14	Flowchart of the navigational risk contour mapping based on inputs of structured data	41
Fig. 15	Result of visualization of risk contour map overlaid on ENC of study area	43
Fig. 16	Four main objects and criteria in route planning	45
Fig. 17	Conceptual diagram of risk gradients for comparison	46
Fig. 18	Five-tier scale system for relative comparison of each object and its ideal goal (bold)	48
Fig. 19	Flowchart of the entire object-oriented route planning process	50
Fig. 20	Pseudo code of defining direction as quadrant	51
Fig. 21	Risk contour map with Pdep and Parr for defining direction	52
Fig. 22	Projection of routes based on the suggested algorithm in the study area	56

List of Figures

Fig. 23 Pseudo code of projecting the ship' s route	57
Fig. 24 Combination case as ${}_3C_2$ among three derived reference points	58
Fig. 25 Conceptual diagram of identified reference points between departure and arrival point for generalization of combination	59
Fig. 26 Pseudo code of route planning as per analysis of objects	60
Fig. 27 Use of Pascal' s triangle for generalization of analyzing portions of object in route planning algorithm	61
Fig. 28 Newly visualized risk contour map reflecting changed condition	66
Fig. 29 Results of numerical simulations for object-oriented route planning as per each object made for maximized portion under the default condition (straight lines) and the changed condition of weather and tidal height (dashed lines)	67
Fig. 30 Tracks of three-day AIS data from GICOMS database in the area	69
Fig. 31 Tracks of filtered AIS data matching the modeled ship and other conditions such as dynamic data and voyage data in the study area	70
Fig. 32 Polygonal boundary of AIS tracks for evaluating the used routes	71
Fig. 33 Result of evaluation of the used routes by statistical AIS data according to a five-tier scale of each object	72
Fig. 34 Result of evaluation of the used routes by statistical AIS data according to reflected portions of each object	73
Fig. 35 Result of selecting each object' s portion as median of AIS data	74
Fig. 36 Sea condition data received from Taean tidal station	77
Fig. 37 Charted diagram of both original and accident route on the risk contour visualized by reflection of the ship' s data in accident	78

List of Figures

- Fig. 38** Comparison of navigational traffic risk along distance and its first derivative81
- Fig. 39** Analysis of the navigational traffic accident to find out causes according to involved objects in the given case study82
- Fig. 40** Charted diagram of both original and accident route on the risk contour visualized by the ship' s data in accident (New Zealand)84
- Fig. 41** Analysis of navigational traffic accident using graphical method85
- Fig. 42** Integration on ECDIS using 3D-based training and simulation materials ...86
- Fig. 43** Mock-up design of integrated Google map and risk contour map on ECDIS ...87



A Study on the Development of Object-oriented Route Planning Technique for Smart Navigation based on Risk Contours

Jeong, Min Gi

Department of Coast Guard Studies

Graduate School of Korea Maritime and Ocean University

Abstract

Route planning in maritime transportation is a key to safe, efficient, and smart navigation in different environments. Conventionally, routes have been planned by operators using empirical and qualitative methods mainly focusing on efficiency. This study proposes an object-oriented route planning technique to objectively and quantitatively determine the routes of vessels in accordance with an operator's intentions.

First, the navigational traffic risk is assessed based on a model of a ship. Next, a risk contour map is visualized by structuring the navigational traffic risk's data consisting of absolute danger, hazard factors, and influential factors, which is a framework of the route planning. Finally, the object-oriented route planning could be modeled with the use of the safety, the efficiency, the convenience, and the ability of navigation as main objects of route planning. The proposed technique assesses each object by making an analysis of cumulative risk per distance, total distance, the number of waypoints, and risk gradient of derived routes. The technique proposes object-oriented routes by

utilizing its algorithm, projecting routes based on contour lines, and combining reference points. To verify the proposed technique, this paper carried out numerical simulation case studies, actual AIS data evaluation of model ships, and analysis of navigational traffic accidents not only on the west coast of Korea, but also on the coast of New Zealand. The result of this study shows that the proposed technique can suggest object-oriented routes depending on a user's purposes, and quantitatively assess the focused objects of the current routes used by vessels and the cause of the previous navigational traffic accidents. Therefore, the object-oriented route planning technique can improve the existing method to be more systematic and quantitative, which contributes to smart navigation based on the user's intentions and the future autonomous navigation.

Accordingly, this study is composed of five sections and each section is structured as follows. Section 1 covered introduction including the background, purpose, scope and method of this study. In section 2, the related works and studies were analyzed in a systematic categorization so that the trend and focus of previous methods can be understood, thus bringing about the necessity and the scope of the proposed technique in this study. In section 3, Risk contour mapping frame work was carried out by structuring the essential data and visualizing the risk contour map based on the experimental area and ship. In section 4, as a core part of this study, the object-oriented route planning technique was conceptualized by introducing four main object of the route planning. Then, the algorithm was developed on the risk contour mapping, so that the proposed technique can derive various options. In section 5, the result of numerical simulations and applications of the proposed technique was suggested for the sake of verification.

KEY WORDS : Navigational traffic risk; Object-oriented; Risk contour; Ship route planning; Smart navigation

스마트 항해를 위한 등리스크 곡선 기반 객체 지향 항로 설정 기술 개발에 관한 연구

정 민 기

한국해양대학교 대학원

해양경찰학과

초 록

해상 교통에서 적절한 항로 계획, 선정은 다양한 해상 환경에서 안전하고, 효율적이며 스마트한 항해 달성을 위해 필수적이다. 기존의 항로들은 주로 효율성 측면에 초점을 맞추어, 경험적이고 정성적인 방법에 기반하여 운항자들에 의해 계획되었다. 본 연구에서는 운항자의 의도, 목적에 따라 객관적이고, 정량적인 방법으로 항로를 설정할 수 있도록 등리스크 곡선 기반 객체 지향 항로 설정 기술을 제안하였다.

첫째로, 선박의 항로 상 해상교통 리스크를 대표 선박을 활용하여 정량적으로 평가하였다. 둘째로, 항로 설정 기술의 기본 단계로서 절대요소, 위험요소, 영향요소로 데이터를 구조화하여 등위험도 곡선 개념 도입을 통해 입체화, 시각화 하였다. 마지막으로 안전성, 효율성, 편리성, 항해 요구능력성의 네 가지 항로 설정 파라미터를 고려하여 객체 지향 항로 선정 기술 모델을 개발하였다. 본 기술에서 각각의 목적 객체를 단위 거리당 누적 위험성, 항정 거리, 변침점의 수, 선택항로의 리스크 정도력이라는 요소 분석을 통해 평가한다. 따라서, 본 기술의 제안된 알고리즘과 등리스크 곡선 기반 항로 작도, 참조지점의 조합을 통하여 객체 지향 항로를 제시한다. 해당 기술을

검증하기 위하여 한국 서해안 실험해역에서 수치 시뮬레이션, AIS data에 기반한 통계적 평가 및 뉴질랜드 연안을 포함한 항로 기인 해상교통사고의 사례적 평가를 수행하였다. 연구의 결과로, 제안된 항로 선정 기술은 운항자의 의도에 따른 객체 지향 항로를 제시할 뿐만 아니라 현재 선박들이 사용하고 있는 항로 및 해상교통 사고 원인을 정량적으로 평가하는 데 활용할 수 있음을 확인하였다. 그러므로 본 기술은 항로 설정 방법을 더욱 체계적이고, 정량적인 방법으로 개선하여 사용자의 목적과 미래의 자율운항선박의 항해를 위한 스마트 항해 실현에 기여할 것으로 기대된다.

본 논문은 5개의 장으로 구성되어 있으며 각각은 다음과 같다. 제 1장에서는 연구의 배경, 목적, 범주 및 방법에 대한 도입을 언급하였다. 제 2장에서는 관련 선행 연구를 분석하여 체계적 방법으로 분류를 통해 종래의 항로 설정 방법들의 경향 및 초점을 파악하였고, 본 연구에서 제안된 기술의 필요성과 연구 범주에서 당위성을 확인하였다. 제 3장에서는 항로 설정의 기본 기술로서, 실험해역에서 실험선박을 활용하여 해상교통 위험요소 데이터를 구조화하여 해상교통 리스크 평가 및 등리스크 곡선을 시각화 하였다. 제 4장에서는 본 연구의 핵심 장으로서, 객체 지향 항로 기술을 네 가지 목적 객체를 사용하여 개념화되었고, 다양한 항로 옵션을 제공하기 위해 등위험도 곡선 상에서 알고리즘을 개발하였다. 제 5장에서는 제안된 기술을 통한 수치 시뮬레이션과 활용도 분석을 통해 연구 결과를 평가하였다.

KEY WORDS : Navigational traffic risk 해상교통 리스크; Object-oriented 객체 지향; Risk contour 등리스크 곡선; Ship route planning 항로 설정; Smart navigation 스마트 항해

Chapter 1. Introduction

1.1 Background and Purpose

Despite efforts to prevent navigational traffic accidents at sea, a majority of accidents continuously have occurred over the past few decades. It was analyzed that almost 80% of navigational accidents result from the inappropriate operation related to navigation (Equasis, 2016; United Nations, 2017). This trend seems more significant not only in that the maritime transportation takes up more than 90% of global trades, but also in that the sizes of fleets keep increasing.

As for the navigational traffic accidents, in the event that a vessel either does not follow an original route plan or does not even plan a proper route at the initial stage, the vessel might be in a dire trouble. Sometimes, the accidents are so catastrophic that the results are deleterious to the whole society as well as to the affected area (Hetherington et al., 2006; Pedersen, 2010).

Even if there were many cases regarding the unexpected accidents, the route planning strategies of vessels still have been conducted in a conventional manner (Swift, 1993; Lee et al., 2018). In other words, there have been no specific standards for navigating officers to decide how far away the ship's course is supposed to be from the obstructions, islands and so on. To make matters worse, those officers are apt to just follow or slightly modify the predecessor's routes;

Furthermore, without verification, they comply with the captains' order with regard to making a decision on routes.

In addition, the previous studies of which topics are related to the route planning, normally have focused on efficient and economical purposes. To be specific, the studies mainly try to plan the routes that reduce fuel consumption, time taken for a voyage, and distance of the leg. One of the limitations of these studies was that the safety had been established as a precondition, resulting in relative ignorance of comprehensive consideration of the route planning. Moreover, commercial softwares developed for route planning also have a tendency of concentrating on the purpose of efficiency and economy by applying a weather routing system. These route planning methods do not necessarily indicate that the suggested routes are optimal in the corresponding situations, because the purpose or navigating conditions significantly vary depending on the operators (Bijlsma, 2001, 2002, 2004, Szlapczynski, 2005, 2011; Lee, 2005; Larson, *et al.*, 2006; Kobayashi, Asajima and Sueyoshi, 2011; Roh, 2013; Guinness *et al.*, 2014; Andersson, 2015; Yoo, Choi and Lee, 2015; Kang *et al.*, 2015; Vettor and Soares, 2016; Yoo and Kim, 2016; Lee *et al.*, 2018; Jeon, 2018).

According to recent studies, it has been reported that the use of geographic data and information as per the context should be taken into consideration for the sake of more reasonable decision makings. Particularly, Riveiro et al. (2018) recommended to apply these data concerned with meteorological, oceanographic, and other necessary factors in order to quantitatively approach a method on finding alternative routes for navigation.

Therefore, this study developed an object-oriented route planning

technique, which ultimately realizes the fit-for-purpose, quantitative and objective decision makings on maritime navigation in a smart way. First of all, risk contour maps were developed so that the risk assessment's paradigm can be shifted from discrete analysis to continuous analysis as curves. Next, based on the risk contour as a framework, the object-oriented route planning method was suggested to overcome the conventional route planning. The proposed technique would be so beneficial owing to a novel approach to the route planning that this study not only helps for operators to smartly plan an objective route but also contributes to wider applications as evaluation of past track of ships, analysis of navigational traffic accident, integration with electronic navigational charts (ENCs) for training, and development of innovative methods for fully autonomous navigation in the future.

1.2 Scope and Method

This study is comprised of total five sections and organized as follows. Section 2 analyzed related literatures so that fundamental information and knowledge about route planning can be acquired. The surveyed literatures contain phase of navigation, phase of route planning, general knowledge regarding risks in connection with navigational traffic accidents. This section systematically categorized the related works in accordance with purposes of navigation in order to bring about the necessity of a new approach to the route planning.

Section 3 conceptualizes risk contour mapping as an essential precedence to establish the object-oriented route planning technique. In this section, using a model of a ship, an experimental area as the west coast of Korea (Janganseong) was designated so that the contour mapping and the further application of the technique can be verified. Also, the

details of the assessment model for navigational traffic risk are specified. The variables as of absolute danger, hazard factors, and influential factors are defined in compliance with the scope of the navigational traffic accidents covered in this study. Using the proposed risk assessment model, the navigational traffic risk indexes were quantified, thus rendering the risk contour mapping visualized as a prerequisite of this study.

Section 4 as the main component of this study describes the detailed technique and its sequential procedures. In order to develop this technique, ultimate factors of the route planning in connection with navigation were determined as four main objects: safety, efficiency, convenience, and ability. Then, the assessment criterion for each object was suggested by making it possible to be analyzed on the risk contour map. Furthermore, an algorithm of the proposed technique was explained in detail, followed by projecting contour-based routes, combining reference points as selection, deriving feasible route options together with the comparison, and finally suggesting the object-oriented route as output. The flow chart of the developed algorithm and pseudo codes were provided to enhance understanding of the whole technique.

In section 5, the results of numerical simulations were provided to verify the proposed technique. Also, wider applications of the proposed technique were validated by three practical case studies: evaluation of routes used by navigators of actual ships based on statistical AIS data acquired from Ministry of Oceans and Fisheries in Korea, systematic analysis of navigational traffic accidents resulting from inappropriate routes in both the study area and other area as New Zealand coast, and integration of the proposed technique with ENC.

Finally, discussion and concluding remarks were described in Section 6 in order to improve the developed technique. In addition, future works has been also suggested to expand this study into an ultimate realization of fully autonomous navigation.

The entire flow chart of the study is illustrated as shown in Fig. 1.



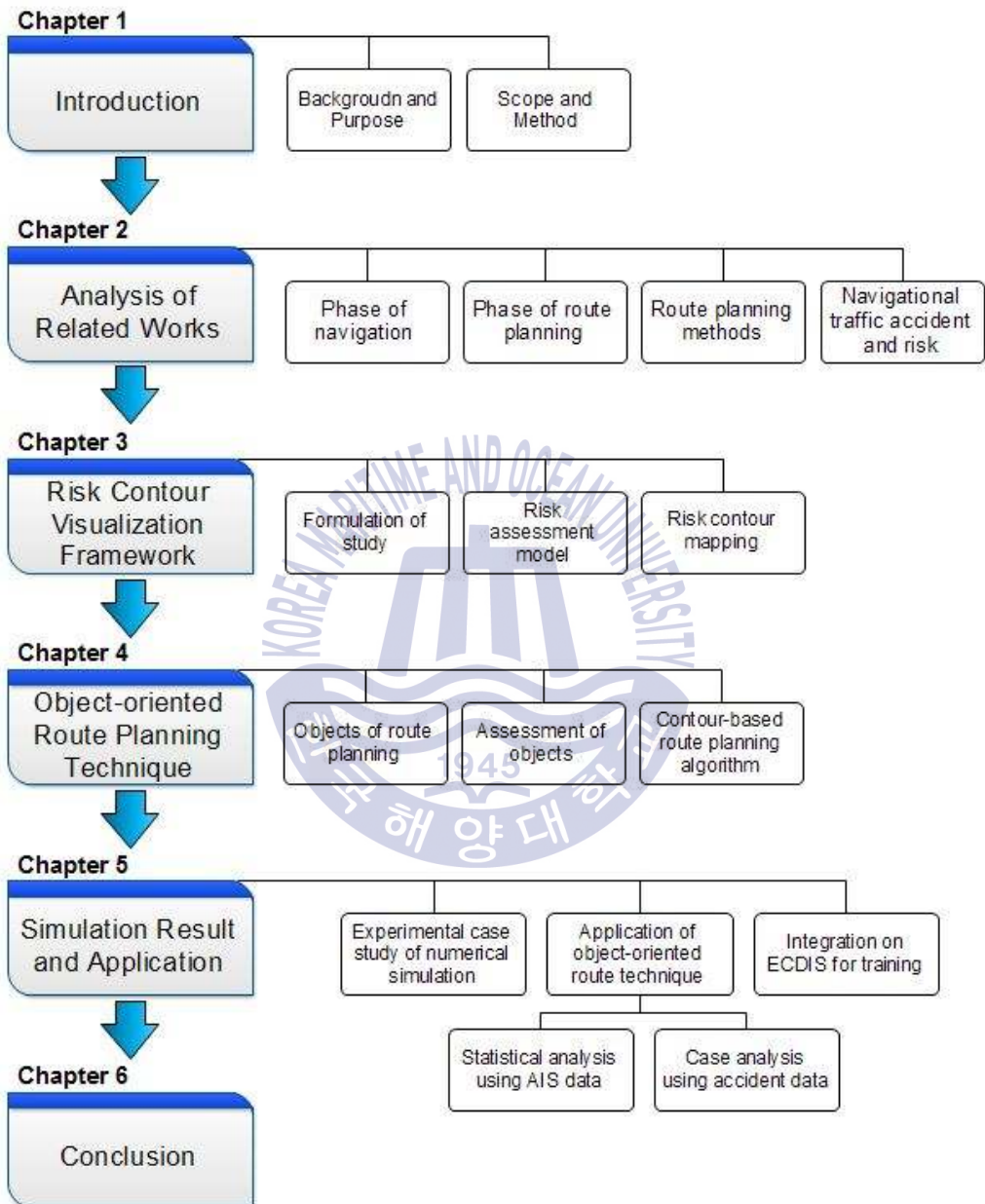


Fig. 1 Organizational flow chart of the study

Chapter 2. Analysis of Related Works

2.1 Phase of navigation

Navigation is defined as “the process of planning, recording and controlling the movement of a craft from one place to another.” (International Maritime Organization, 2001). In general, as Fig. 2 shows, there are four distinct phases of maritime navigation, which are ocean navigation, coastal navigation, harbor approach navigation, and inland navigation; therefore, it is important to recognize what phase the vessel belongs to in order to plan a route suitable for a corresponding phase. The standards on defining the phases can slightly vary depending on documents, but this study adopts the standard from National Imagery and Mapping Agency (2002) and International Association of Lighthouse Authorities (2018).

First of all, ocean navigation is when the vessel is typically outside of the continental shelf and more than 50 NM from the nearest land as open sea. In this phase, now that the vessel is far enough from stationary obstacles or shallow waters, the maritime traffic risks resulting from the hazards are relatively stable at a considerably lower value. This trend can be typically observed by ocean navigation’s operation which requires no additional operators such as a captain or supporters owing to relatively easy stage.

Next, coastal navigation is normally navigating within 50 NM from the

shoreside or within the continental shelf, and the vessel starts to encounter decreasing water depths as well as the emergence of obstacles affecting the navigation. Therefore, the maritime traffic risk generally increases as the ship approaches due to frequent confrontation of hazards ahead of it. In addition, appearance of hazards at this stage is so rapid that fluctuation of risks can be observed. For this reason, the operators begin not only to plot the ship's position more frequently, but also to obtain assistances from additional supports such as systems or manning of watch keepers.

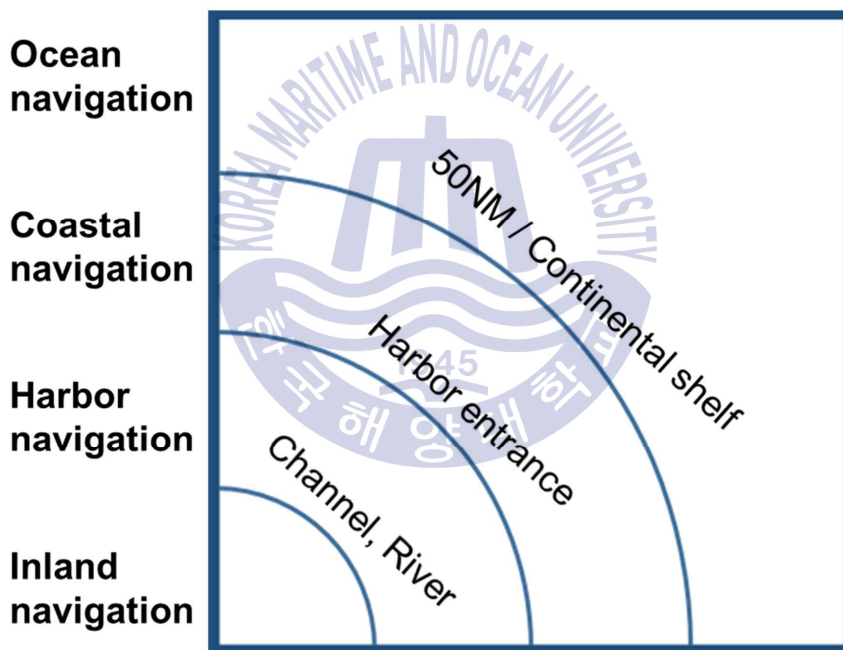


Fig. 2 Conceptual diagram for phases of navigation

Furthermore, harbor navigation represents navigating through harbor entrance as a transition from coastal navigation. In this phase, the vessel is located within more confined waters than coastal navigation, thus requiring more attention and capability of an operator. Due to

many hazards scattered around the ship, the vessel is also guided by a marine pilot who is expert within that region. Hence, the safety objective of navigation is much considered between the coastal and harbor navigation.

Last, inland navigation is navigation stage while passing narrow channels or rivers, which make the ship very close to dangers and impose limitations on its movements. The pilot as well as the ship's operators pay due attention in order to prevent the unexpected accident, and the route plan of the ship should be carefully exchanged between the pilot and the master.

Since the scope and method of the route planning is different from each phase, it is essential to determine which phase a study is intended for to develop the route planning technique suitably. For instance, route planning technique as per the phase of ocean navigation, which mainly focuses on great circle navigation to achieve efficient and economical purposes does not necessarily coincide with the purpose of navigation during the coastal phase.

2.2 Phase of route planning

Route planning is divided into the four main steps as appraisal, planning, execution, and monitoring. Fig. 3. shows these four phases of route planning. Each stage possesses its own significance to ensure a goal of intended navigation. Based on these sequential phases, the operator continuously tries to achieve better navigation by reflecting any changes during the application (International Maritime Organization, 2002b).

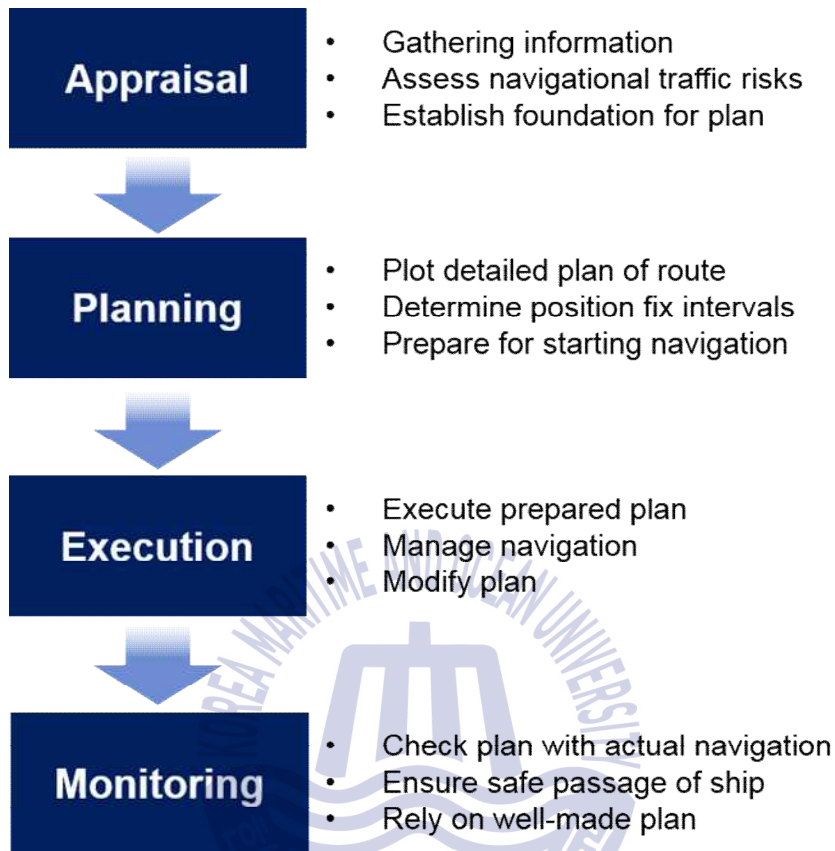


Fig. 3 Four phases of route planning

Above all, the appraisal phase is one of the most fundamental phases in that data or information related to the navigation are accumulated and analyzed in order to identify and evaluate navigational traffic risks. The operator should assess the level of risk properly during this phase, thus establishing a foundation necessary for an optimized option of the route plan for the next phase. Therefore, the operators are urged to utilize the quality-sources of available information as much as possible. These contain navigational charts, including ENCs, technical publications, personal experiences, other useful supports such as Notice to Mariners, and etc.

The passage planning phase refers to actual plotting of courses, determining position fixing intervals, and identifying predicted hazards in order to avoid the assessed risks. Also, the operator concentrates on efficient handling of the courses so as to reduce the unnecessary consumption of fuel or required time. Typically, the planning stage is comprised of filtering out No-Go Areas, clearing margins of safety, identifying navigable areas, charting tracks, marking course alterations and wheel-over positions, and setting up measures in case of any contingencies. Even if the vessel is involved in navigating within the same region, the operator makes sure that route plans should not be the same since the conditions not only from internal factors but also from external factors have been changed.

The execution phase represents carrying out the route plan by making the ship engaged in proceeding to the navigation. During this phase, the following available information should be agreed: Estimated Time of Arrival, traffic conditions, manning of crews on duty watches, briefing on the route plan among concerned officers, voyage preparation from both engine and deck part, and risk management in response to some unexpected situations. Executing a pre-made route plan is not always stable. In other words, the operators are likely to modify the plan in order to flexibly make a better decision in the corresponding situations.

Finally, the monitoring phase is to ensure the vessel is in compliance with pre-made route plan. As a result, the operator should take care of this monitoring phase during the watch in real-time. Monitoring consists of analyzing the current state and moving onto an action as per its result of analysis. For example, the officer on watch confirms the ship's position regularly so that the ship follows the pre-determined track, thus not rendering itself enter dangerous area. Also, the operator

calculates the ship's relative position to the destination, and adjust the speed in order to make a proper ETA without delays. Therefore, these series of actions are predicated on well-made route planning at the appraisal and planning phase.

2.3 Route planning methods

Since route planning is an important step for conducting navigation, a majority of works have been focused on the route planning by using diverse approached under different conditions. The previous works were specifically analyzed based on the categorizing both main purpose of the methods and phase of navigation. Table 1 shows analyses of them using two categorization.

2.3.1 Categorization of route planning methods

First of all, the purposes of the utilized methods were concentrated on its fundamental objectives after all. According to the analysis, the purposes were mainly divided into two: economic and efficient routes, and safe routes. Moreover, the economic and efficient routes vary depending on their specialized sub-categorization as fuel consumption, distance, time, cost, and weather influence, whereas the safe routes show a tendency on avoidance of ships or obstacles located ahead.

Table 1 Structured analysis of works related to route planning

Works	Category of main purpose									Phase of navigation			
	Purpose of efficiency and economy					Purpose of safety							
	Distance	Fuel	Time	Cost	Course change	Weather	Collision avoidance	Obstacle avoidance	Depth	Inland	Harbor	Coastal	Ocean
Bijlsma (2001; 2002; 2004)		○	○			○							○
Lee (2005)	○											○	
Szlupczynski (2005)					○			○			○	○	○
Larson et al. (2006)							○	○		○	○	○	
Kobayashi et al. (2011)		○				○							○
Szlupczynski (2011)	○						○				○	○	○
Roh (2013)		○				○							○
Guinness et al. (2014)				○				○				○	
Andersson (2015)		○	○			○							○
Kang et al. (2015)	○	○	○						○			○	
Yoo et al. (2015)		○				○							○
Yoo and Kim (2016)						○							○
Vettor and Soares (2016)		○	○										○
Lee et al. (2018)	○	○	○										○
Jeon (2018)							○					○	
Eniram (2018)	○	○		○		○						○	○
LG CNS (2018)		○		○									○
StormGeo (2018)	○	○	○	○		○						○	○
Weathernews (2018)	○	○	○	○		○						○	○

2.3.2 Efficiency-based and economy-based route planning

Specifically, within the scope of efficient and economical routes, Bijlsma (2001, 2002, 2004) mainly dealt with computational methods for making a route as minimal-time of transit or fuel consumption during ocean navigation such as a route crossing the Atlantic ocean from Nantucket Shoals to Bishop Rock. Lee (2005) suggested an optimal route decision algorithm based on the closing and thinning technique, followed by a real-coded genetic algorithm with its simulation based on a coastal area. Also, a weather routing method during ocean navigation was proposed in order to reflect ocean currents, wind and waves, thus rendering minimum fuel consumption by the Powell method. Roh (2013) applied a routing method as A*algorithm¹⁾ to suggest an economy-based route for minimized fuel consumption by analyzing the sea state on various oceans. A* algorithm was also utilized by Guinness *et al.* (2014) to present an ice-aware maritime route optimization which reduce associated costs that require consideration of ice conditions and supports of icebreaker at Baltic Sea by effectively avoiding the ice obstacles. In order to obtain a route optimization that modify the routes as per reduced time, reduced wave height, and reduced fuel consumption, a grid search approach and Pareto genetic algorithm were adopted predicated on the scope of weather routing during an ocean voyage. In addition, a weather routing method mainly targeted for fuel-efficient operation of ship was developed by utilizing the Powell method during ocean navigation (Yoo et al., 2015). A path planning algorithm based on machine learning was developed in consideration of dynamic characteristics, i.e., ocean currents of marine vehicles during the ocean

1) In computer Science, A* is a computer algorithm that is widely used in pathfinding and graph traversal, which is the process of finding a path between multiple points, called "nodes" (Source: Wikipedia, 2018).

navigation (Yoo and Kim, 2016). Ship weather routing system focusing on sea-state condition was suggested by modelling a robust multi-objective evolutionary algorithm for the sake of reducing time and fuel consumption (Vettor and Soares, 2016). Lee *et al.* (2018) also proposed a optimization route planning based on a genetic algorithm in order to solve a problem by considering both determination of the path and the speed of a ship.

After analyses of commercial products such as decision making programs for route planning, the same interests of routes can be observed. In other words, Eniram (2018), LG CNS (2018), StormGeo (2018), and Weathernews (2018) concerns about weather routing in order to mainly achieve reduction of distance, fuel consumption, time, cost under the predicted weather conditions in large scales at least during the wide area of coastal navigation or ocean navigation. Therefore, the route planning methods previously developed by regardless of researches or commercial products, show a tendency to focus on the algorithms making the routes efficient and economical as a priority. Within the categorization of efficiency and economy, the methodology per each route also slightly varies depending on the ultimate goals such as distance, fuel, time, cost, course change, and weather effects. However, an essential element of the route planning, i.e. the safety, was considered as an assumption or a subsidiary prior to plotting the route plans. In other words, these planning methods have no standards on managing risks along the route, and have only to suggest routes based on such a precondition that the routes sometimes are abnormal in that they enter the non-navigable areas such as lands, and obstructions.

2.3.3 Safety-based route planning

Even for safety-based route planning methods, Szlapczynski (2005) put forwards an obstacle avoidance method predicated on making the course changes as small as possible. Another approach was intended for collision avoidance with other ships (Szlapczynski, 2011). A path planning method aimed for autonomous navigation of unmanned surface vehicles (USVs) was suggested by the interest of the Navy, other Department of Defense, Department of Homeland Security of the United States in that the real-world environments were reflected for collision or obstacle avoidances (Larson, *et al.*, 2006). Kang et al (2015) applied Electronic Navigational Chart (ENC) to make a route plan primarily in consideration of depth, wrecks, and other obstacles, of which ultimate goals were to minimize the distance, fuel, and time of the courses. Jeon (2018) considered historical statistic data of ship tracks by Automatic Identification System (AIS) as a model of a area nearby South sea of Korean waters, thus rendering routes safe as a prevention of collisions with other vessels.

Nevertheless, there are also limitations in these studies on route planning, because the routes were adjusted continuously when obstacles are encountered at the phase of execution and monitoring. That is, there is relatively low consideration of holistic approach of the route planning from the origin to the destination not by reflecting appraisals in advance and preemptive plans, but by reflecting momentary method of avoidance algorithms. Therefore, these studies were likely to suggest paths from short-term aspects without original routes based on the systematic grounds.

All in all, the analyzed methods do not necessarily represent the optimized routes. Specifically, the efficiency-based and economy-based route planning methods are not the best ones in terms of the

requirements or intentions of navigators under different situations. Moreover, as for the safety-based route planning methods, even if the methods are plausible for preventing accidents in real time, they do not always stand for fit-for-purpose routes that satisfy the users' requirements depending on the situations.

In consequence, in order to propose preemptive routes during the phase of the appraisal and planning, the object-oriented planning technique was proposed in this study. The proposed technique was emphasized on ultimate smart navigation as per different purposes of the users and conditions under the phase of coastal navigation, where the maritime traffic risks tend to significantly fluctuate due to the abrupt change of surrounding environments.

2.4 Navigational traffic accident and risk

In order to quantitatively assess risks related to a ship's route and propose the object-oriented route planning, definition of the risk in connection with accidents is to be circumscribed.

2.4.1 Definition of navigational traffic accident

Definitions of accidents in maritime area can slightly vary depending on approaches. International Maritime Organization (2008) defines marine accidents in terms of any marine casualty or incident, which can be classified by order of severity: very serious marine casualties, serious marine casualties, less serious casualties, marine incidents.

According to Act on the investigation of and inquiry into marine accidents in Korea (Ministry of Oceans and Fisheries, 2018), marine accidents are defined as 14 types. These include collision, contact,

grounding, capsizing, fire, explosion, sinking, lost, engine failure, propulsion system failure, steering gear failure, auxiliary failure, flooding, and others.

Similarly, accidents can be divided into 13 types by Korea Maritime Safety Tribunal (Korea Maritime Safety Tribunal, 2018a). There are collision, contact, grounding, fire/explosion, sinking, engine failure, propulsion system failure, steering gear failure, human injury, degradation of safety, degradation of operation, and lost.

In addition, Korea Coast Guard (Korea Coast Guard, 2014) defines the type of accidents as collision, grounding, contact, sinking, flooding, fire, explosion, engine failure, propulsion failure, steering failure, auxiliary failure, facility failure, winding of floating objects, degradation of operation, loss of direction, human injury, marine pollution, and others.

Nevertheless, accidents from the point of view related to maritime traffic can be defined by the approach of maritime traffic engineering (Kristiansen, 2005; Park et al., 2008). They can be divided into collision, grounding, contact, fire/explosion, sinking, capsizing, human injury, flooding, weather damage and etc., in terms of traffic accidents or technical accidents.

Based on the definition of the engineering approach, in order to be consistent with the approach of route planning, navigational traffic accidents were defined as grounding, contact, capsizing, and sinking, which are caused by navigational operation connected with stationary obstacles. Therefore, dynamic obstacles such as other ships or other moving objects were excluded because the developed route planning technique was predicated on the phase of appraisal and planning, prior to carrying out a voyage.

2.4.2 Definition of navigational traffic risk

According to the previous studies by Li *et al.* (2012), Zhang *et al.* (2016), and Zhen *et al.* (2017), risk assessments concerned with traffic in maritime area can be broadly divided into three categories.

First of all, as for risk modeling in accordance with the general definition of risk, the risk value can be obtained by multiplying the probability of an accident and its consequence. For example, Chin and Debnath (2009) devised an evasive action according to calculated by probabilistic level of collision and its damage. Goerlandt *et al.*, (2015) developed Collision Alert System (CAS) with case studies, using fuzzy expert system in order to assess the collision risk during ship-ship encounters.

Next, the statistical analyses of traffic accidents were conducted in order to derive the risk. Mazaheri *et al.*, (2015) assessed grounding frequency based on ship's traffic and waterway complexity, using a large amount of data regarding traffic density as well as previous accidents. Also, port traffic risk in Hong Kong port was assessed by a negative binomial regression model based on sufficient data as 660,426 ships from 2001 to 2005 (Yip, 2008).

Moreover, non-accident data can be applied in order to quantify necessary risks at sea. This case is specifically attributable to insufficient data of previous accidents together with the amount of traffics accumulated. In general, this approach of risk is primarily based on quantification of index interconnected with the occurrence of accidents. Risk indexes can be beneficial to not only finding out a dangerous situation, but also preventing a ship from involving in an accident

predicted by correlation with the derived indexes (Zhen et al. 2017; Yoo, 2018).

In this study, navigational traffic risk is defined as the risk index, which is basically associated the probabilistic approach in terms of navigational traffic accidents such as grounding, contact, capsizing and sinking. Since the route planning technique aims to prevent a ship from entering a risky area by eliminating any unsafe situations, the consequential factor was assumed as a constant. In other words, the navigational traffic risk in this study directly means the probabilistic risk expressed in index within a designated area.



Chapter 3. Risk Contour Visualization Framework

3.1 Formulation of Study

3.1.1 Experimental area (Janganseong)

An experimental area in this study has been designated in order to effectively verify the object-oriented route planning technique: to assess navigational traffic risk, to visualize risk contour, and to apply route planning method. Among many regions, the ‘Janganseong’ area located on the west coast of Korea peninsular (shown in Fig. 4) has been designated because it satisfies the requirements of the study. The detailed description of the study area is provided in Fig. 5 as a nautical chart.

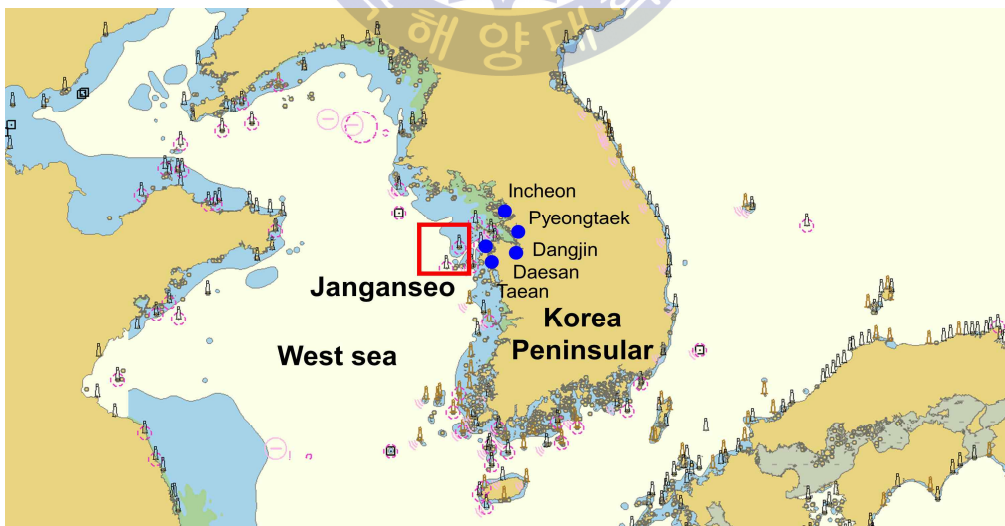


Fig. 4 Experimental area for study (Janganseong)

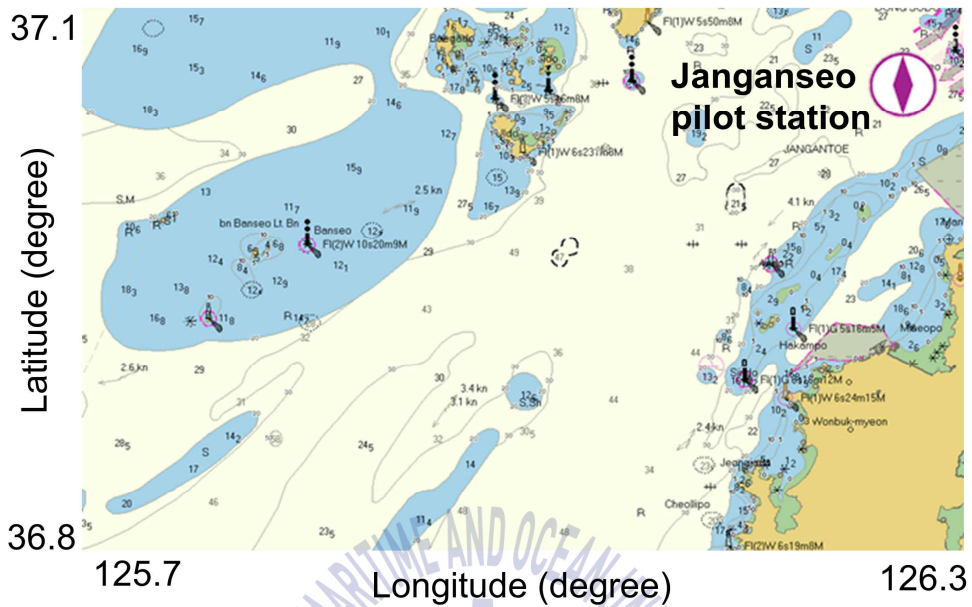


Fig. 5 Detailed description of study area on nautical chart

The reasons why Janganseong was selected for study area are as follows. First, there is no pre-determined traffic directions by a system such as a traffic separation scheme and a traffic lane. In the event that there are pre-determined directions of the ships' traffic, it is difficult to apply the route planning technique for validation due to compliance with them. Therefore, Janganseong is one of the ideal areas, where the route planning technique can be practically evaluated without interruptions.

Next, Janganseong region is one of the most bustling regions around the coast of Korea. Specifically, the region is always busy with ships calling in and out of nearby ports, that is, Pyeongtaek, Incheon, Dangjin, Daesan and etc. (Korea Hydrographic and Oceanographic Administration, 2018). For this reason, the object-oriented route planning technique could be fundamentally applied in the area with a large amount of

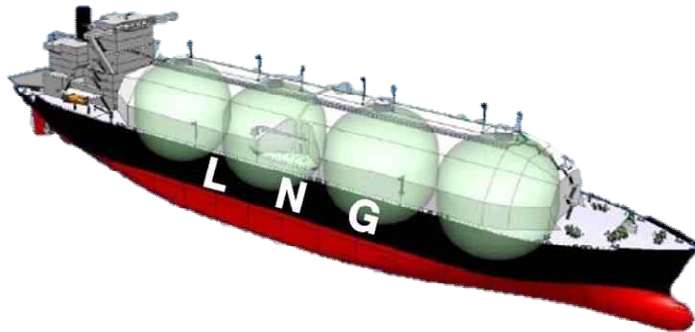
required data for the sake of evaluating both the past tracks of AIS and the case study for analyses of navigational traffic accidents.

Last, the area has a good condition of environmental characteristics, including tidal heights and weather conditions. In this area, the difference of tidal heights between low and high tide normally shows significant variance as almost 8 meters. Also, diverse sea conditions with strong currents and winds, and poor visibilities due to fog can be naturally observed. On top of that, there are ocean data buoys which were deployed (such as Taean port ocean data buoy) so that the actually acquired data at sea could be inputted to the system of the proposed technique.

3.1.2 Experimental ship

As a model of a ship, a specific type and size have been selected. Liquefied Natural Gas (LNG) Carrier was a main model of the study in that it is one of the large-sized vessels transiting the corresponding area (Korea Gas Corporation, 2009a, 2009b). Also, LNG Carriers have relatively higher standards for the safe operation of the route planning and its navigation. Within the area, due to the main LNG ports as Pyeongtaek and Incheon, they are also regularly observed, enabling a sufficient amount of necessary data. Fig. 6 describes the specific details of the modeled ship. Among the LNG carriers managed and operated by Korea Gas Cooperation (KOGAS) calling the ports, Moss type 135K LNG carrier takes up the highest portion of the fleet (Javanmardi *et al.*, 2006; Korea Gas Corporation, 2009a, 2009b). Moreover, LNG carriers usually have a regular shape and size under the capacities of cargo tanks. In other words, without the significant variance regarding physical characteristics, the LNG carrier was an ideal model for easy validation

of the technique on a common scale.



Source: Trade Arabia, 2018

Type	135K Class LNG
Length overall(L.O.A) [m]	288.77
Breadth [m]	48.2
Gross Tonnage	113,998
Draft [m]	11 Even Keel
Block Coefficient	0.68
Proceeding Speed [knots]	15

Fig. 6 Principal specification of the experimental ship

3.2 Risk Assessment Model

3.2.1 Data structure of risk assessment

In order to assess the navigational traffic risk in an area, data affecting the risk were structured in accordance with the analyses of technical references, previous studies, past accidents, and experts' opinions (Kristiansen, 2005; Ulusçu *et al.*, 2009; Jeong *et al.*, 2017).

Fig. 7 illustrates the structure of the data for navigational traffic risk: absolute danger, hazard factor, and influential factor. All data in a spatial area were geometrically analyzed and evaluated using ENC (Jeong *et al.*, 2018a, 2018b, 2018c, 2018d)

Among the variables that affect navigational traffic risk, the absolute danger is defined as the non-navigable area with a relation between the actual water depth and the ship's maximum draft including squat and its margin. The hazard factor is defined as a factor within the navigable area, which directly affects the cause of accidents. After the non-navigable area is filtered out as per the absolute danger, the hazard factor is comprised of the hazardous depth and the obstacles, which stand for stationary obstacles. Then, the hazardous depth is defined in detail as the minimum water depth within the navigable area, whereas the obstacles are subdivided into the artificial or natural obstacles. The natural obstacles are the ones created naturally, such as wreck, obstruction, foul, rock, islet, coral reef and any naturally generated obstacles on ENC. However, the artificial obstacles are ones created by human beings, such as buoy, beacon, fishing ground, platform, lighthouse, wind farm, and any man-made obstacles on ENC.

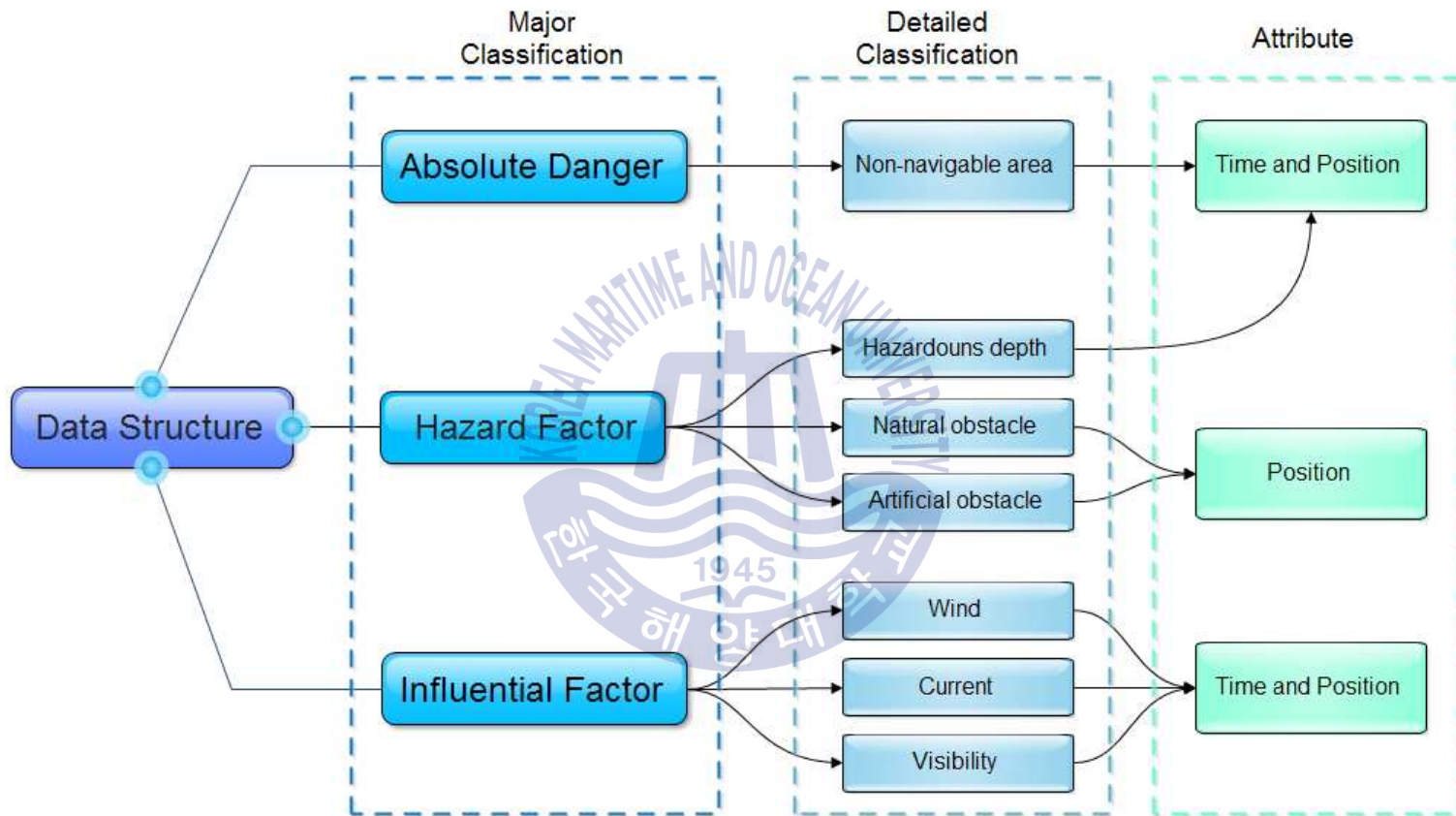


Fig. 7 Data structure as variables for assessment of navigational traffic risk

Last, the influential factor represents the sea condition (wind, current, and visibility) in the corresponding area that have an indirect effect on the cause of maritime traffic accidents, in contrast with the hazard factor.

3.2.2 Assessment of maritime traffic risk

The navigational traffic risk for route planning in this study can be formulated by the calculation of following Equation. (1) by the analysis of the previous studies (Jebsen and Papakonstantinou, 1997; International Maritime Organization, 2002a; International Association of Marine Aids to Navigation and Lighthouse Authorities, 2009; Mazaheri, 2009; Kim and Lee, 2012; Lee and Kim, 2013; Mazaheri et al., 2015; Zhen, Riveiro and Jin, 2017; Jeong et al., 2018a, 2018b, 2018c, 2018d; Korea Maritime Safety Tribunal, 2018b)

$$NTR_i = f(area_i) = [H_{i,water} \ H_{i,obs}] \begin{bmatrix} A_{i,water} \\ A_{i,obs} \end{bmatrix} \cdot w_{i,condi} \quad (1)$$

where the subscript i is the identification numbering of the unit area, NTR_i is the index of the navigational traffic risk within the area I [NTR], $H_{i,water}$ is the hazard factor's index calculated by the hazardous depth in relation with the depth of water and the ship's maximum draft, $H_{i,obs}$ is the hazard factor's index calculated by the obstacles, $A_{i,water}$ is the weight coefficient for the geometric size of the non-navigable area in relative comparison with that of the unit area, $A_{i,obs}$ is the weight coefficient for geometric size for the boundary of the obstacles in relative comparison with that of the unit area, and $w_{i,condi}$ the weight coefficient of the influential factor as a sea condition.

Each input variable is calculated based on a matrix of hazard and

influential factors according to Table 2. In this study, the default index of the *NTR* was designated as the values ranging from 1 to 20, without the influential factors as the sea condition, $w_{i,condi}$. After influential factors are reflected to initial *NTR* value, *NTR* is finally derived by considering all required factors.

Table 2 Elements affecting the safety of maritime traffic

Type		Hazard factor		Influential factor		
Variable		$H_{i,water}$	$H_{i,obs}$	$w_{i,condi}$		
				$S_{i,wind}$	$S_{i,current}$	$S_{i,visibility}$
Criterion		Hazardous depth (h/D)	Obstacle cohesion	Wind	Current (c/V)	Visibility
Rating	5	< 1.2	< 20 %F	≥ 21 m/s	≥ 0.4	< 0.099 NM
	4	< 1.5	< 40 %F	< 21 m/s	< 0.4	< 0.486 NM
	3	< 2.0	< 60 %F	< 14 m/s	< 0.3	< 1.0 NM
	2	< 3.0	< 80 %F	< 8 m/s	< 0.2	< 5.5 NM
	1	≥ 3.0	≥ 80 %F	< 3.3 m/s	< 0.1	≥ 5.5 NM

h : the minimum depth in navigable area [m],

D : the maximum draft of a ship [m],

%F: the unit of obstacle cohesion,

c : the speed of current [knots],

V : the speed of a ship [knots].

3.2.3 Unit area for risk assessment

A unit area for assessing the navigational traffic risk is determined by definition of position fixing interval, which is the criterion that ‘a ship does not run into a danger during the interval between fixes’ (Oil Companies International Marine Forum, 2016) as per the ship’s navigational safety.

Fig. 8 represents an example of an actual position fixing interval used by modeled ships from a LNG operating company in this study area according to the route plan. This definition means that the ship will not encounter hazards to make sure the ship is safe in case of heading to any directions from the previous position.

Specifically, the unit area has a circular shape with a radius, which can be calculated by the multiplication of position fixing intervals and the ship's transit speed. The conceptual diagram of the unit area for assessing the navigational traffic risk is shown in Fig. 9. In this study, the position fixing interval for determining the unit area was applied as 6 minutes not only because of the value adopted by most of route plans of LNG operators under contract with KOGAS, but also because of analysis of the study area in relation to the ship's transit speed and topographical features.



Unit area radius = Position fix interval·Ship's speed

Fig. 9 Conceptual diagram of unit area for assessment

3.2.4 Filtering absolute danger

Prior to designing a route plan on a designated area, it is fundamental to identify navigable areas (Swift, 1993). Thus, it is required to filter out non-navigable area as the concept that the ship never enters. The absolute danger defined as non-navigable area in this study can be found by the ship's maximum draft and actual depth in the target area.

In order to calculate the ship's maximum draft, a formula to determine the maximum squat has been adopted from Barrass (2004) as described in Equation (2),

$$SQT_{\max} = \frac{C_b \cdot V^2}{100} \quad (2)$$

where SQT_{\max} is the maximum squat [m], C_b the block coefficient of the ship, V the speed of the ship [knot]. Then, the calculated value of the squat is to be added to the ship's original draft, and the margin for the non-navigable area should be reflected in accordance with companies' operation manuals and technical guidance. In this study, the margin as 20 % was applied as per the values by LNG operators under contract with KOGAS and professional guidelines (Swift, 1993; PIANC, 2014; Hyundai Merchant Marine, 2018)

Afterwards, the non-navigable area is excluded from depth data of the whole region. As shown in Fig. 10, the depth data were composed of raw data as bathymetry measurement by Korea Hydrographic Office in order to enhance accuracy and resolution quality, because depth data on nautical charts are already segregated by equal curves as depth lines, which does not reflect intended accuracy to find the navigable area.

▲	Long (°)	x	Lat (°)	y	Depth (m)	z
1	129.55844		40.67901		26	
2	133.95627		39.4684		1440	
3	126.10782		35.8513		28.5	
4	130.34834		33.72077		23	
5	129.80677		33.55321		23	
6	129.39975		33.31114		8.6	
7	130.88541		37.43651		258	
8	131.28599		42.35293		286	
9	132.07329		43.15129		13.2	
10	122.43623		32.12522		21	
11	128.57164		34.56831		55	
12	129.67418		36.01385		128	
13	129.44919		36.5454		5.5	
14	129.73535		36.72019		5.3	
15	129.25393		37.50801		148	

⋮

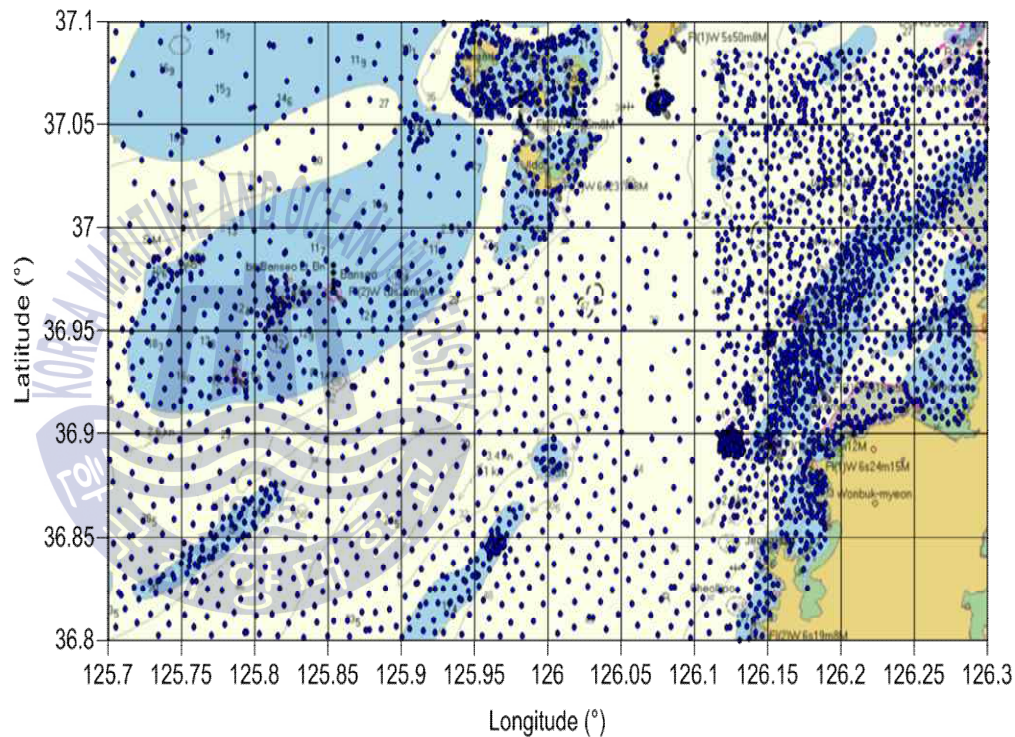


Fig. 10 Use of raw bathymetry data from Korea Hydrographic Office

3.2.5 Quantification of hazard factor

After input of the hazard factors, the rating of the hazardous depth is scaled in accordance with the Table 2. In particular, the ratio as comparison between the ship's draft and the minimum depth level within the navigable area is utilized to quantify it.

On the other hand, the rating of the obstacles is scaled depending on the obstacle cohesion which is spatially assessed based on clustering analysis (Kanungo *et al.*, 2002; Lee *et al.*, 2014; Lee, *et al.*, 2017). The conceptual diagram of this geometric analysis is described in Fig. 11.

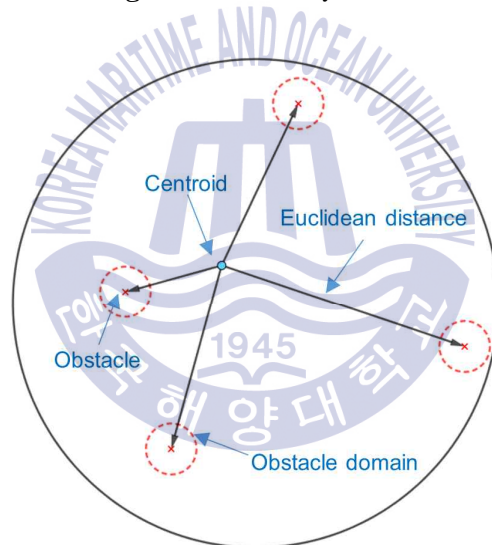


Fig. 11 Analysis of obstacles within the unit area using clustering

The quantification is followed by identification of both the number of obstacles and the cohesion tendency within the unit area, as relative comparison with the semi-diameter of the unit area and the average distance between obstacles and the centroid (mean position of obstacles). The obstacle cohesion is calculated by Equation 3,

$$\begin{aligned}
cohesion_i &= \frac{1}{N(obs)} \cdot \sum_{P(x,y) \in area_i} d(P,C) \\
&= \frac{1}{N(obs)} \cdot \sum_{P(x,y) \in area_i} \sqrt{(x-x_{i,c})^2 + (y-y_{i,c})^2}
\end{aligned} \tag{3}$$

where $cohesion_i$ is the obstacle cohesion in unit $area_i$, $N(obs)$ is the number of existing obstacles in the area [EA], P is the position of an obstacle in the area as coordination (x,y) , C is the position of the centroid in the area as coordination $(x_{i,c},y_{i,c})$, and $d(P,C)$ is the Euclidean distance on the plane of two dimensions. Note that the unit of obstacle cohesion value is [%F], where F is the position fixing interval as the semi-diameter of the unit area (i.e., circle). The obstacle cohesion represents the concentrated characteristics of the inter-obstacle distance in the spatial area.

With regard to coefficients of Equation (1), incremental percent weights for the hazard factor, i.e., hazardous depth (H_{water}) and obstacles (H_{obs}) are calculated respectively as $A_{i,water}$ and $A_{i,obs}$ by the relative ratio of the non-navigable area within the unit area. To be specific, $A_{i,water}$ is quantified by the size ratio between the unit area and the non-navigable area due to the water depth, whereas $A_{i,obs}$ is quantified by the size ratio between the unit area and the non-navigable area due to the domain of obstacles. In case that the obstacles are polygonal shapes, $A_{i,obs}$ can be just calculated by the domain that each vertex circumscribes as a boundary. However, in case that the obstacles are certain points such as buoys, obstructions, wrecks and etc., $A_{i,obs}$ can be calculated as the obstacle domain for the safe clearance. This safe clearance stands for the margin, which the ship should never enter. In this study, the obstacle domain was designated by the criterion as the overall length of the ship, which is adopted by the review of technical

studies and the survey of experts (Pietrzykowski and Uriasz, 2009; Inoue, 2013; PIANC, 2014).

3.2.6 Quantification of influential factor

An influential factor in Equation (1) is basically calculated by determining the sea condition effect on the default condition of the navigational traffic risk, indirectly increasing the possibility of accidents. This factor is based on the statistical data analysis of navigational traffic accidents from 2011 to 2017 (Korea Maritime Safety Tribunal, 2018a); Moreover, it is calculated by using the concept of a nominal index of the sea condition effect, which has a motif from the ship's slip calculation (Bialystocki and Konovessis, 2016; Jeong *et al.*, 2018d), as Equation (4),

$$\max(\omega_{condi}) = 1 + \frac{N(total) - N(net)}{N(net)} = 1 + \frac{N(diff)}{N(net)} \quad (4)$$

where $\max(\omega_{condi})$ is the nominal maximum weight coefficient of an influential factor, $N(total)$ is the total number of navigational traffic accidents during the observed period [EA], $N(net)$ the net number of the navigational traffic accidents not influenced by sea condition [EA], and $N(diff)$ is the difference between the total number and net number of navigational traffic accidents [EA].

The collected and analyzed data is shown in Table 3. Among total 786 cases of navigational traffic accidents, the sea condition was involved in the occurrence of the accidents as 155 cases, which means that 631 cases of the accidents were not involved in the sea conditions.

Since the influential factor is sub-divided into three variables as wind, current, and visibility, according to the accident data, its value in Eq (1) is obtained by the calculation using Eq. (5) in connection with Equation (4), as the actual effect of sea condition,

$$\omega_{i, \text{condi}} = 1 + \frac{1}{100} \cdot [\rho_{\text{wind}} \quad \rho_{\text{current}} \quad \rho_{\text{visibility}}] \begin{bmatrix} S_{i, \text{wind}} \\ S_{i, \text{current}} \\ S_{i, \text{visibility}} \end{bmatrix} \quad (5)$$

where ρ_{wind} , ρ_{current} , and $\rho_{\text{visibility}}$ are the relative comparison as portions among influential factors, and $S_{i, \text{wind}}$, $S_{i, \text{current}}$, and $S_{i, \text{visibility}}$ are the rating index of wind, current, and visibility, respectively analyzed by input data as shown in Table 2.

Table 3 Elements affecting the safety of maritime traffic

Traffic accident data	$N(\text{total})$	$N(\text{net})$	$N(\text{diff})$
Number of accidents	786	631	155
$\max(w_{i, \text{condi}})$	1.2456		
Category of influential factor	Wind	Current	Visibility
Number of accidents due to sea condition	99	37	19
Ratio	0.6387	0.2387	0.1226
Portion index (ρ_{wind} , ρ_{current} , $\rho_{\text{visibility}}$)	3.1373	1.1725	0.6021

In addition, after analysis of total 786 cases, according to the statistical data, the portion values were computed by multiplying each ratio of the three elements among influential factor by 4.91 in order to comply with the value of $\max(w_{i, \text{condi}})$ in Equation (4), on the condition that the rating

of the wind, current and visibility is the maximum rating as 5 respectively. Available data for calculating the influential factor in this study were inputted by actual observations from ocean buoys or tidal stations as shown in Fig. 12 (Korea Hydrographic and Oceanographic Administration, 2018).

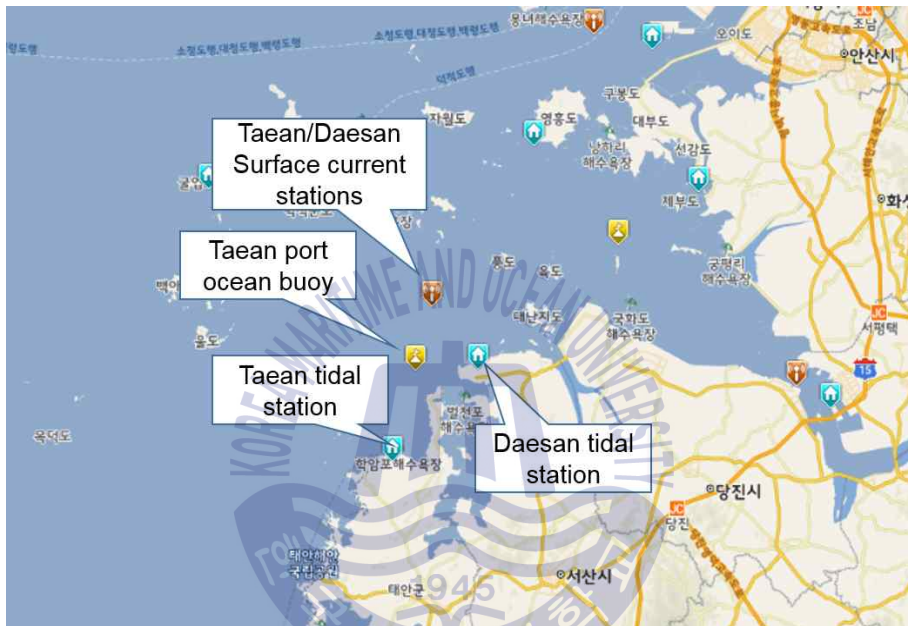


Fig. 12 Available data from observatories for influential factor

3.3 Risk contour mapping

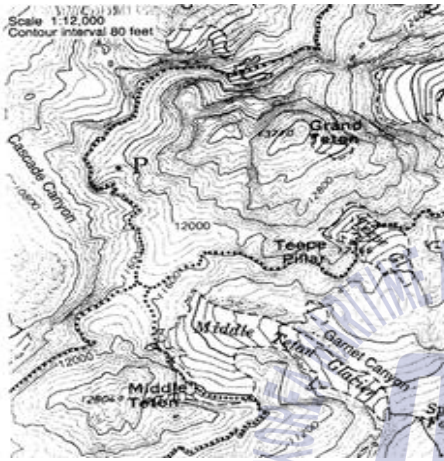
3.3.1 Use of contours

A typical contour map is a topographic equal curves as a representation of the vertical level of the Earth's surface along the cross section (Cronin, 1995; Chen *et al.*, 2004). In addition to topographic mapping, the contours have been widely utilized in diverse areas. For example, another common contour mapping can be seen in the use of barometric pressure to illustrate high or low atmospheric pressures and their movements (Casola and Wallace, 2007). Also, magnetic fields can be drawn as curve so as to describe an invisible area of magnetic forces, according to their strength (Hoburg, 2004). As an application to the marine area, one of the most common uses for contours is oceanographic bathymetry (Danilo and Melgani, 2016). Above all, the strong advantages of these contour maps (shown in Fig. 13) can not only make what are not visible as visible lines, but also help people understand both the distribution and the strength of a drawn subject (Li and Liu, 2010; Chen *et al.*, 2014).

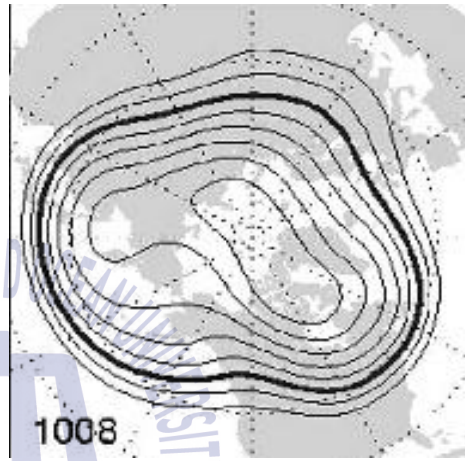
3.3.2 Concept of risk contour

In a similar way, the concept of the risk contour has been developed in order to describe and visualize the level of navigational traffic risks at sea as the curves (Jeong *et al.*, 2017). In other words, after assessing the navigational traffic risk in the unit area at Section 3.2, a risk contour mapping is expressed as two-dimensional curves, using the kriging interpolation method. Kriging is defined as an interpolation method that serves as a geostatistical gridding that has been utilized by

diverse literatures and fields owing to its powerfulness (Matheron, 1973; Kumar, 2007). Hence, the navigator can identify and grasp the navigational situation in terms of the risk contour; furthermore, the risk contour can support the smart navigation of ships based on technical methodologies on it (Jeong *et al.*, 2018a, 2018b, 2018c, 2018d).



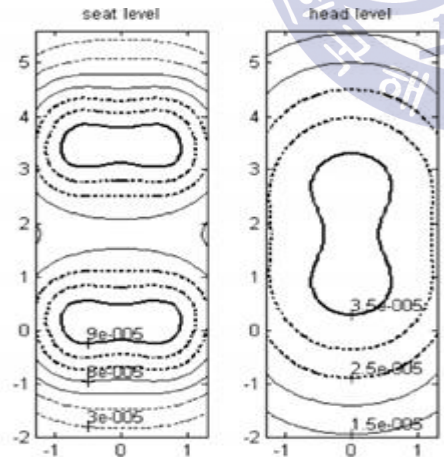
Source: Cronin, 1995



Source: Casola and Wallace, 2007

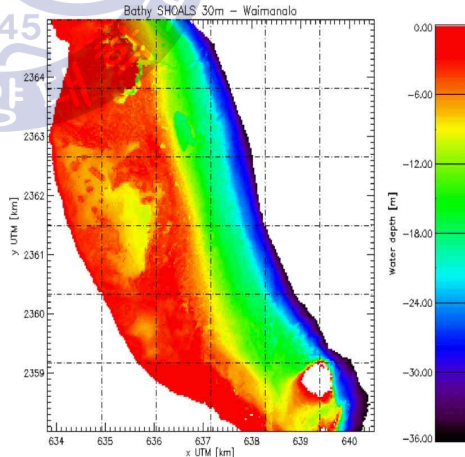
(a) topographic contour

(b) barometric contour



Source: Hoburg, 2004

(c) magnetic field contour



Source: Danilo and Melgani, 2016

(d) bathymetry contour

Fig. 13 Examples of contours in diverse areas

3.3.3 Procedure of risk contour visualization

Risk contour visualization follows sequential steps comprised of spatial identification, geometric analysis, quantitative assessment of the navigational traffic risk, and mapping as equal curves on ENC. The holistic view of the steps is illustrated in Fig. 14.

The steps can be specified as the following procedures: First of all, data and variables are inputted through the connection with ENC and navigational equipment. At this stage, inputs are sub-categorized in order to be systematically applied to the system as of the data structure, that is, absolute danger, hazard factor, and influential factor. Next, after identification of the absolute danger, the non-navigable area is determined and filtered out in red color. Third, the assessment of navigational traffic risk in unit area is conducted. As a result, the risk contour visualization is formulated as an overlay on ENC. This risk contour mapping as a cell on ENC is designed to be overlaid or hidden depending on the situations and users.

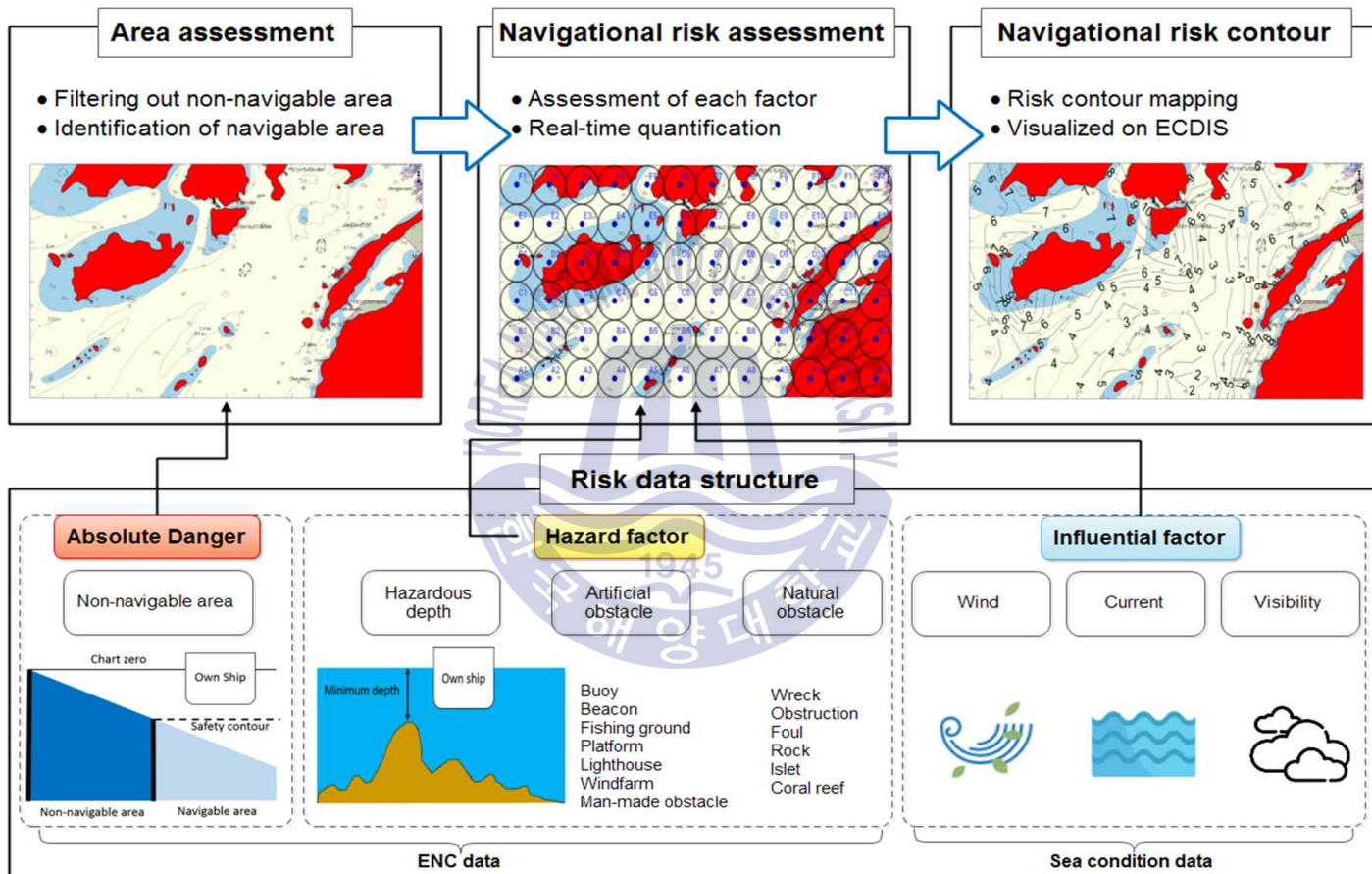


Fig. 14 Flowchart of the navigational risk contour mapping based on inputs of structured data

3.3.4 Novelty of risk contour visualization model

The visualized risk contour has a significant novelty in addition to specific merits. The result of risk contour model is shown in Fig. 15 as an expression of visualized contours for entering the port of Pyeongtaek. First, it analyzes scattered and dispersed hazard data at sea, consequently expressing them as continuous and connected information. This contour shifts the paradigm of the navigational traffic risk assessment from discrete spatial analysis to a continuous method as curves with novelty. In addition, the risk contour enables the navigational traffic risk that is originally intangible and invisible to be quantified and visualized. Next, the operator can be supported when it comes to a decision making, such as contour-based route planning, which eventually meets the requirements of the operator's intentions and preferences. Furthermore, using the risk contour, the new concept in the literature can be obtained in terms of the risk gradient, a derivative of the risk value, and cumulative risks. The newly developed concept offers new types of information which can be utilized for further study. Last, it is expected that the risk contour is conducive to the wider application such as statistical analysis of past tracks using AIS data and objective evaluation of navigational traffic accidents (discussed in Section 5) in addition to the main part of this study as object-oriented route planning (discussed in Section 4).

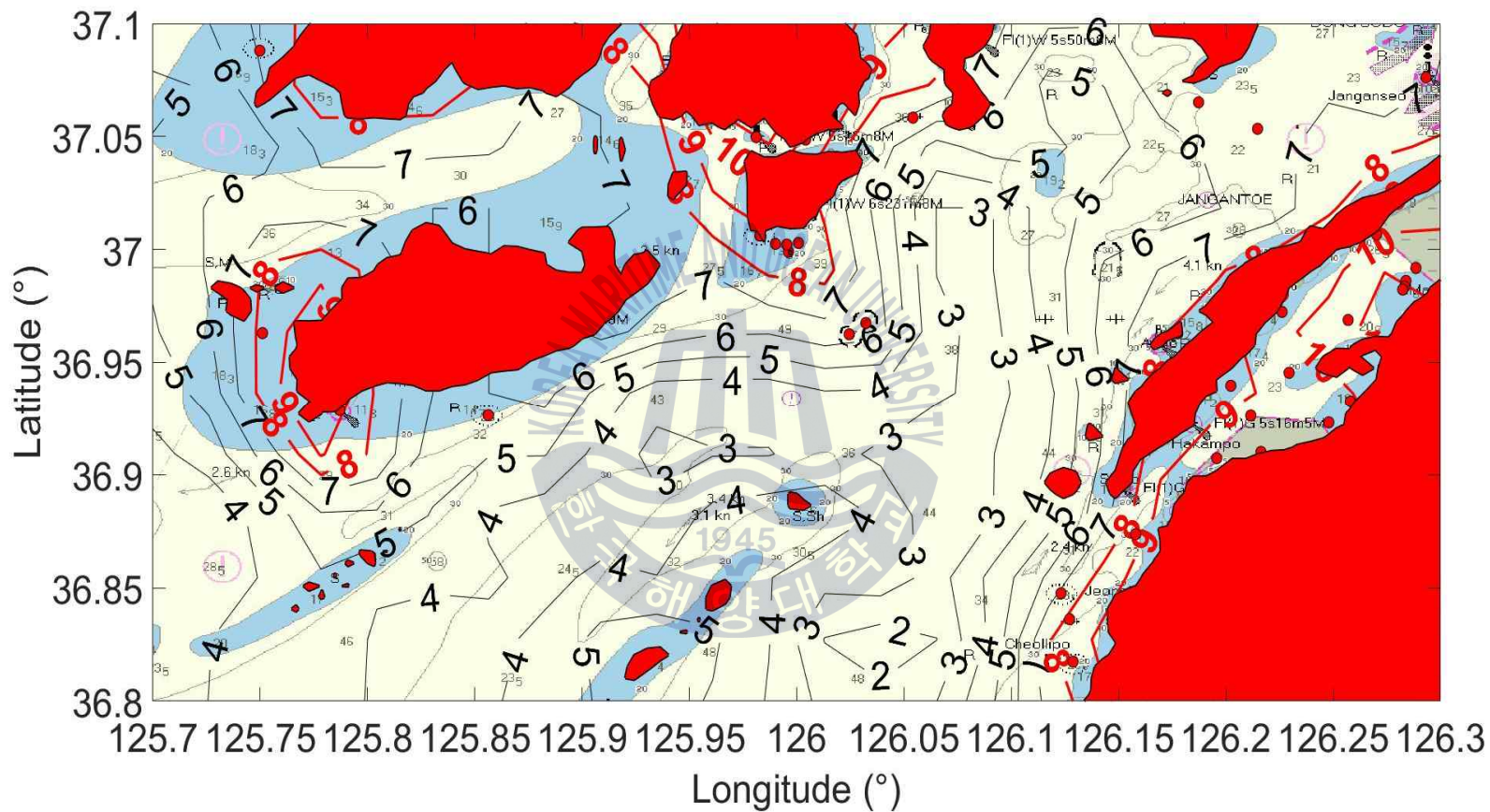


Fig. 15 Result of visualization of risk contour map overlaid on ENC of study area

Chapter 4. Object-oriented Route Planning Technique

4.1 Objects of route planning

According to the comprehensive reviews of technical references, previous works and studies, and experts' brainstorming (Roh, 2013; Guinness *et al.*, 2014; Andersson, 2015; Kang *et al.*, 2015; Lee *et al.*, 2018, Jeong *et al.*, 2018b, 2018c, 2018d), the ultimate goals of navigational route planning could be defined as four main criteria: the safety, efficiency, convenience, and ability of navigation. The emphasis on each goal of the route planning might significantly vary depending on the respective method of the operators. However, it has an important role in determining the various options and purposes of the route planning. Therefore, in order to quantitatively analyze each goal as an object and plot a route for smart navigation in the corresponding circumstances, the definition of objects were established (shown in Fig. 16).

Above all, the safety object is defined as the criterion on how a ship can engage in a safe navigation along the planned route by preventing the cause of navigational traffic accidents. Next, the efficiency object stands for the criterion on how the ship can expedite the navigation along the route in an efficient method. Moreover, the convenience object is defined as the criterion on whether the ship has to frequently alter the course, thus making the operation of ship maneuvering easy.

Last, the required ability of navigation means a criterion of whether the navigation can be conducted by both the ship and the operator in that the ship has sufficient device and availability of operation, or the operator has enough knowledge, experiences, and supports to carry out the navigation on the route.

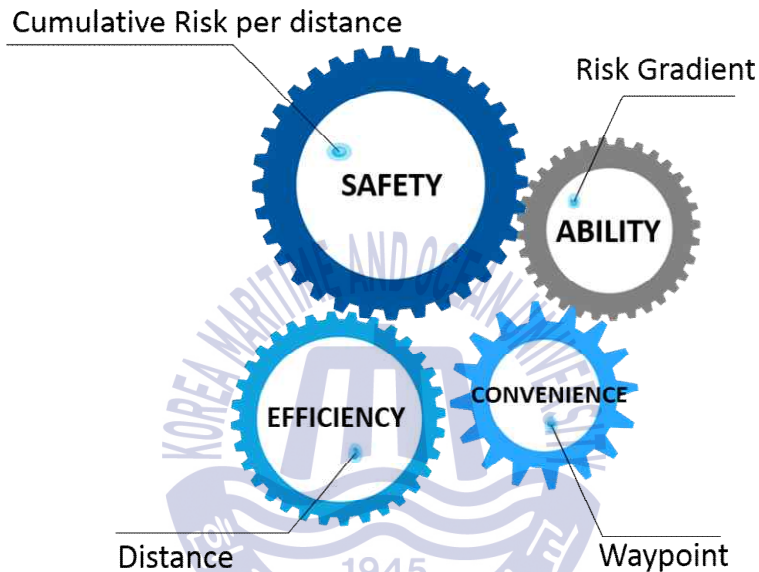


Fig. 16 Four main objects and criteria in route planning

4.2 Assessment of objects

In this study, standards for the assessment and measurement of objects have been determined based on the risk contour map as a fundamental framework in accordance with the definition in Section 4.1.

The safety object is assessed by the cumulative risk per distance along the planned route on the risk contour map as a horizontal plane, which is calculated by Equation (6),

$$CRD = \frac{\int_{P_{dep}}^{P_{arr}} NTR}{dist} \quad (6)$$

where CRD is the cumulative risk (integration of NTR) per distance [NTR/NM], P_{dep} is the position of the departure point, P_{arr} is the position of the arrival point, and $dist$ is the total distance along the route from P_{dep} to P_{arr} . Now that the cumulative risk per distance is inversely proportional to the safety of the route due to the increased possibility of navigational traffic accidents, the low value of it stands for the quite safe route.

Next, the efficiency object is determined by the total distance along the suggested route. As the distance parameter is also inversely proportional to the efficiency, the measurement between the distance and the efficiency follows the same correlation as the safety object.

Third, the convenience object is defined by the number of waypoints on the route. It has the proportional relationship same as the aforementioned safety and efficiency object.

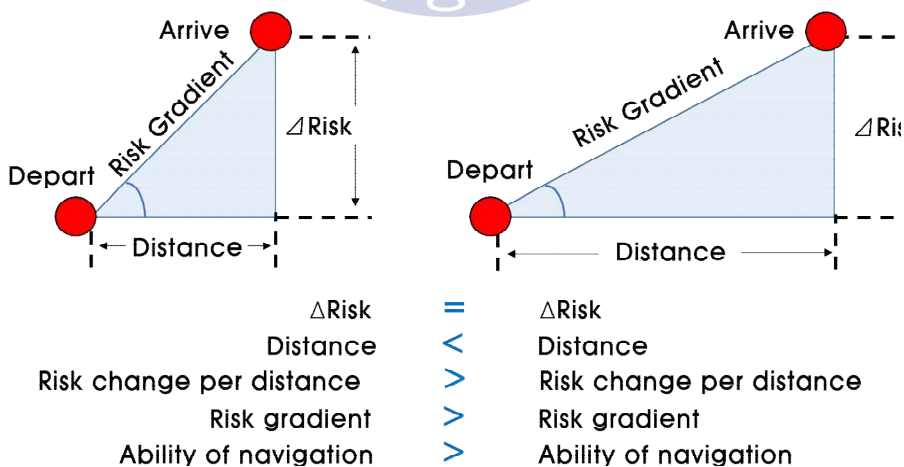


Fig. 17 Conceptual diagram of risk gradients for comparison

Last, the ability of navigation has a definition of the average risk gradient on the risk contour map. The concept of the risk gradient can be compared to that of climbing on a mountain along topographic altitude contours. For example, in the event that the interval between the altitude contour is fixed, the distance between the interval shows the steepness of the gradient, thus requiring an appropriate ability of mountain-climbing depending on that gradient. Likewise, navigational routes determined by a steep or gradual gradient on a risk contour map require different abilities of the operation. In other words, as the ability of navigation rely on the steepness of the risk gradient, the steeper gradient means the higher ability of navigation, which can be supported by additional equipment, professionalism of operators, and back-up human resources such as a master, pilot, or other officers. Fig. 17 illustrates details of the concept. Consequently, the ability of navigation can be calculated as described in Equation 7,

$$Avg.Grd = \frac{|NTR(P_{arr}) - NTR(P_{dep})|}{dist} \quad (7)$$

where *Avg.Grd* is the average risk gradient along the selected route [Δ NTR/NM], $NTR(P_{dep})$, and $NTR(P_{arr})$ are *NTR* index at point P_{dep} and P_{arr} , respectively. Contrary to the other objects, the risk gradient has directly proportional to the ability of navigation.

In summary, each object of route planning is determined and quantified by a certain criterion based on the risk contour map. In addition to the measurement of the each object, a five-tiered rating based on relative comparison of each object as per all possible routes from a departure point to an arrival point has been adopted as shown in Fig. 18. The relative comparison uses the minimum and maximum

value of each object among feasible routes derived from the proposed technique. The tiered rating also follows the proportional relationships as what is previously analyzed. Therefore, three objects as the safety, efficiency, and convenience have an inversely proportional relationship to the assessed criteria, whereas the ability objects shows a directly proportional relationship. Based on these relationships, the ultimate ideal goal of an object in a certain route was marked in bold.

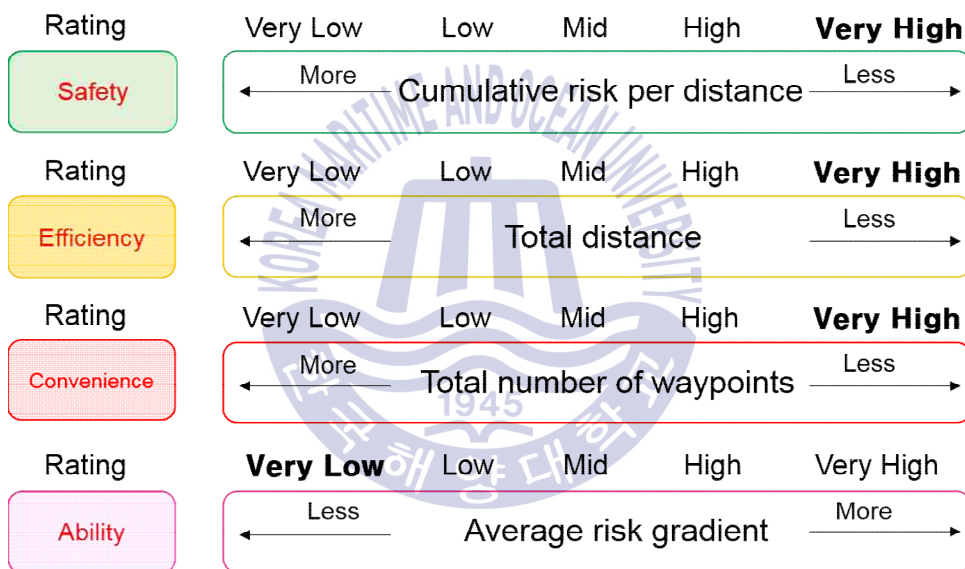
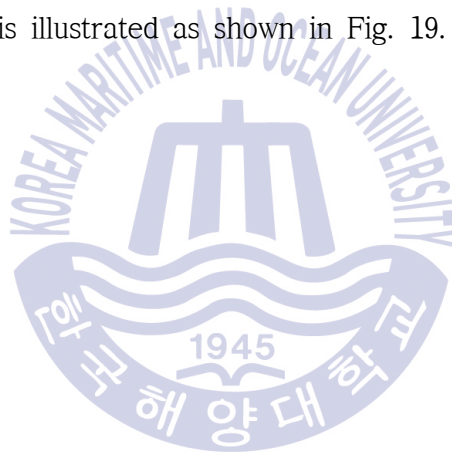


Fig. 18 Five-tier scale system for relative comparison of each object and its ideal goal (bold)

4.3 Contour-based route planning algorithm

In this study, the object-oriented route planning technique is proposed with four main objects for the smart navigation of a vessel on the risk contour map (Jeong *et al.*, 2018b, 2018c, 2018d). The proposed technique was developed by application of algorithm codes in MATLAB. The hardware environment of the running system was based on 3.30 GHz Intel Core i3 CPU processor and 8 GB DDR4 RAM. As the object-oriented route planning is accomplished in sequential orders, the flowchart of the entire algorithm regarding the object-oriented route planning technique is illustrated as shown in Fig. 19.



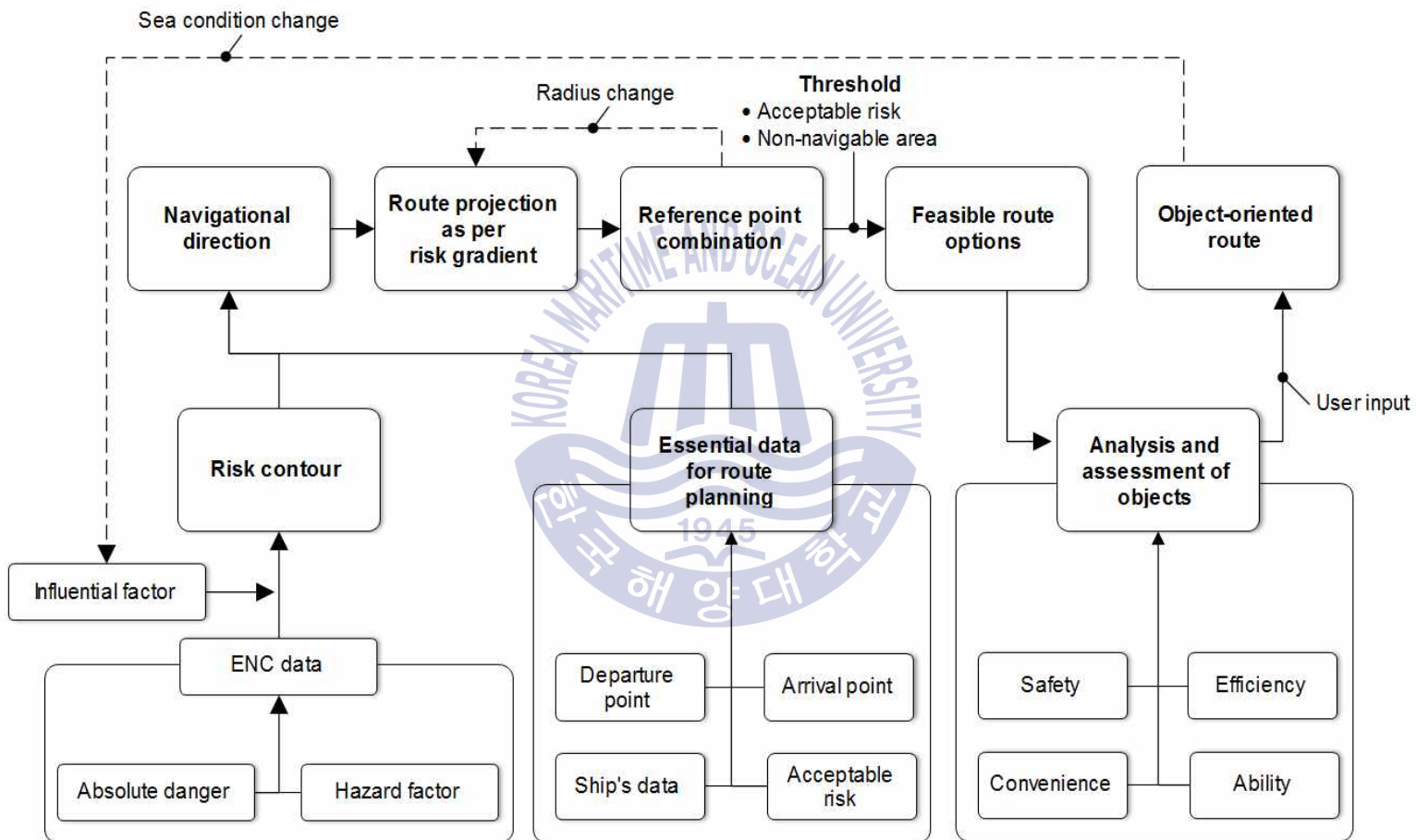


Fig. 19 Flowchart of the entire object-oriented route planning process

4.3.1 Defining navigational direction

As for the object-oriented route planning technique after the visualization of the risk contour is completed, the essential data input should be conducted by the operator. Hence, the user enters the departure and arrival point, maximum acceptable risk for the safety margin, and the ship's principal data such as dimensions. The proposed technique, then, determines the direction of intended navigation in order to derive a proposed route in the further steps. The pseudo code developed to define the direction of the navigation is represented as shown in Fig. 20.

Algorithm 1: Define direction

Read : Risk Contour map on Electronic Navigational Chart
Input : P_{dep} , P_{arr}
Output : Quadrant of route direction to be proposed

- 1 Define θ as direction of bearing from P_{dep} , P_{arr}
- 2 Quadrant $\leftarrow 0$
- 3 **for** $n = 1$ to 4 **do**
- 4 | **if** $90 * (n - 1) \leq \theta < 90 * n$ **then**
- 5 | | mark Quadrant as n
- 6 | **end**
- 7 **end**
- 8 **return** Quadrant

Fig. 20 Pseudo code of defining direction as quadrant

To be specific, after the risk contour map is loaded on ENC, first, the navigational direction between the departure point (P_{dep}) and the arrival point (P_{arr}) is defined by identification of a quadrant. The quadrant is a directional region as four components, which equally separate bearings from 000 degrees to 359 degrees. This step supposes that the direction of a suggested route after application of the technique should be within

the identified quadrant. Without this assumption, an infinite possible number of cases that can go to P_{arr} . For example, courses that go from backwards against the destination and then comes back to forwards direction can exist; Furthermore, there might be more serious cases having zig-zag directions. In these cases of suggested routes are fairly far from the actual route planning on board the vessel in reality.

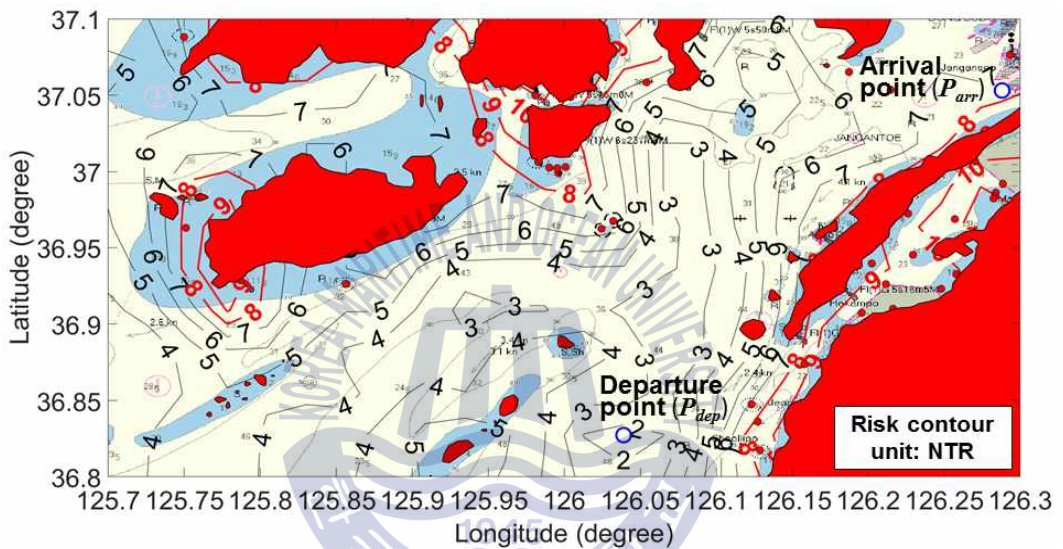


Fig. 21 Risk contour map with P_{dep} and P_{arr} for defining direction

Fig. 21 shows the result of the navigational area together with departure and arrival point, which are loaded on ENC. The illustrated figure is predicated on the assumption of the default condition of external elements, i.e., no effect of both tide and weather. The reason was to validate the proposed technique under initial condition, then apply the changed condition like what the entire methods of this study were designed.

As per the inputted value, P_{dep} , P_{arr} , the non-navigable area due to the water depth as 15 meters (shown in red polygon regions), and the

non-navigable area due to the maximum acceptable risk as 8 NTR (shown in red line contours) was identified on the risk contour map. The non-navigable area due to the water depth was excluded based on the calculation of the maximum draft, including a squat effect of the modeled ship. Also, the non-navigable area due to the maximum acceptable risk was intended threshold for the minimum safety margin that leaves discretions on the operators. P_{arr} was plotted as GPS position of the Janganseong pilot station, while P_{dep} was randomly determined among the ship's position of entering directions as Southwest from the destination. This case demonstrates that the returned result of the quadrant is defined as the first quadrant. Thus, the navigational direction of route plans to be proposed should lie in the first quadrant, including the routes' subordinate legs. As a result of defining direction algorithm, the proposed technique is able to determine the direction no matter what conditions are or no matter where P_{dep} and P_{arr} are located.

4.3.2 Route projection based on risk gradient

The route projection method of this study was motivated by a projection method adopted by topographic engineers, when designing a road on a mountain or network connections for wind farm stations (Rogers, 2005; Gu *et al.*, 2015). Those engineers determine the route based on the desired gradient on the topographic contours. Specifically, they spot intersections of contour lines by drawing the value of the desired gradient prior to the destination; the connecting lines of the spotted intersections are deduced as the possible route projections. However, instead of topographic contours adopted by other studies regarding geographic purposes, this study utilized the risk contour, the novel concept as the framework, in order to project a ship's route at

sea based on ENC.

The modeled ship's preliminary route projections could be conducted using the available risk gradients from P_{dep} to P_{arr} . In detail, as calculation of the navigational traffic risk's displacements between P_{dep} and P_{arr} , the test of available risk gradients was performed so as to check whether the value of the risk gradient is technically applicable in that area, resulting in a large number of simulations. In the event that the interval of the risk contour is fixed as mentioned in Section 4.2, the desired risk gradient is expressed as a radius of the circle from the origin to the intersection on the next contour level as an adjacent one. Therefore, the simulations of this *Radius value* were conducted by considering the interval of the visualized risk contour, the distance of adjacent risk contour lines, and the vessel's characteristic such as size and maneuverability. In other words, the desired risk gradient for the route projection is concerned with the ability object in Section 4.2. The derived circle as per the risk gradient is defined as the gradient circle, of which concept was applied by references (Rogers, 2005; Gu *et al.*, 2015). The related calculation is expressed in Equation 8,

$$R = \frac{\Delta_{contourint}}{Grad} \quad (8)$$

where R is the radius of the gradient circle as the desired distance between two adjacent risk contour lines [NM], $\Delta_{contourint}$ is the interval of contours as displacement of NTR between two adjacent contour lines { NTR }, and $Grad$ is the desired risk gradient of the route [NTR/NM].

Now that $\Delta_{contourint}$ is designated as a constant value once the risk contour map is visualized, $Gradient$ is determined by $Radius$ as a sole factor that has an influence. It was also postulated that the risk

contour's surface has a continuous change across the plane in order to apply the suggested algorithms. Also, extreme values of *Radius* are to be excluded in that too small or too large *Radius* is not proper enough to have an intersection from P_{dep} owing to the pre-test of applicability of *Radius* at the initial stage. Then, the proposed route projection algorithm is technically programmed as sequential structure described as follows (Jeong *et al.*, 2018b, 2018c, 2018d):

Sequence 1) A circle with *Radius* is drawn from P_{dep} .

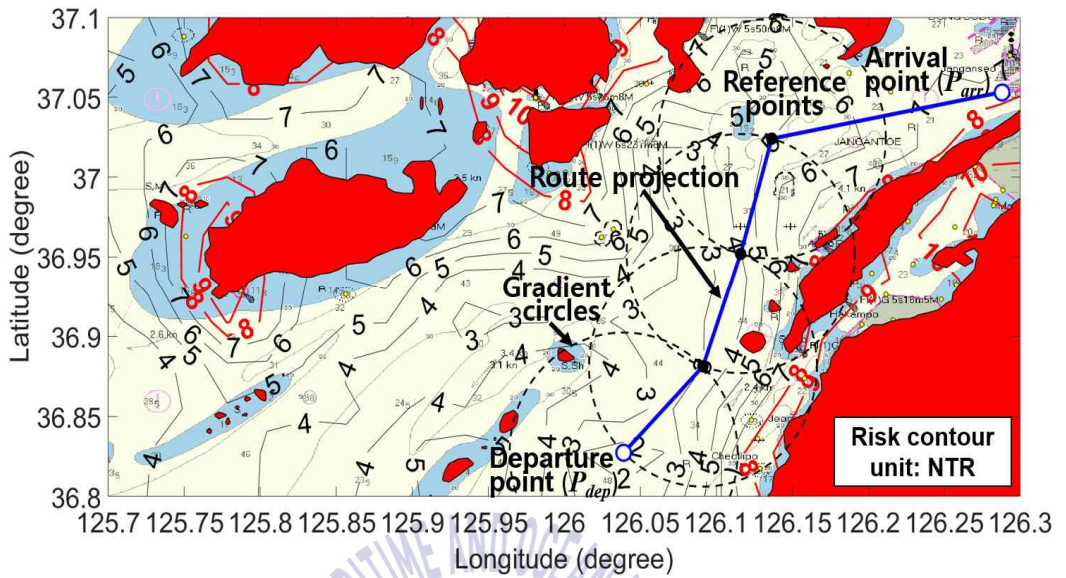
Sequence 2) Identify any intersection between the circle and the risk contour of the next level.

Sequence 3) In case that an intersection is found, the point is named as a reference point, and a segment line is connected from the center of the circle to the control point. A continuous process starting from sequence 1 are repeated from the identified control point as a new center of a circle. In case that an intersection is not found during the process, a direct line to P_{arr} is connected.

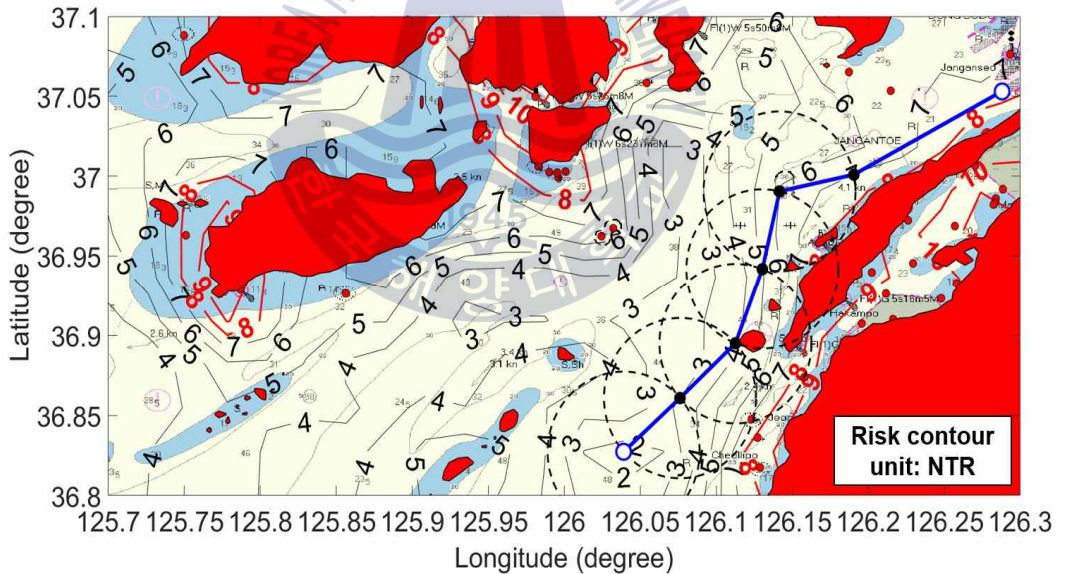
Sequence 4) After the last route segment reaches P_{arr} , the procedure is completed.

Sequence 5) Check the availability of the derived preliminary route.

For explanation of these sequences, Fig 22 shows the preliminary route projection by the proposed sequences. In the event that there are plural intersections with the adjacent contour line from the center of the circle, all the possible routes are analyzed by separating the case of the line segment depending on each intersection. On the other hand, in the event that no intersection exists during the process, a direct line to P_{arr} is derived as the route segment, as described in Sequence 3.



(a) radius of gradient circle as 4.5 NM relatively low ability of navigation



(b) radius of gradient circle as 3 NM with relatively high ability of navigation

Fig. 22 Projection of routes based on the suggested algorithm in the study area

Algorithm 2: Make the ship's route projection

Read : Risk Contour map on Electronic Navigational Chart
Input : *Gradient, Radius*
Output : Route projection for corresponding *Radius*

- 1 Define i as label of each contour level from P_{dep} to P_{arr}
- 2 **for** $Radius = \text{minimum}(Radius)$ to $\text{maximum}(Radius)$ **do**
- 3 | draw circle with $Radius$ from P_{dep}
- 4 | mark refPoint as intersection between circle and adjacent risk contour
- 5 | add refPoint to Set(refPoint)
- 6 | **for** $i = \text{minimum}(i)$ to $\text{maximum}(i)$ **do**
- 7 | | **if** circle from refPoint intersect with contour($i+1$) **then**
- 8 | | | mark intersection as refPoint
- 9 | | | add refPoint to Set(refPoint)
- 10 | | **else**
- 11 | | | draw direct line from refPoint and P_{arr}
- 12 | **end**
- 13 | connect route from P_{dep} via Set(refPoint) to P_{arr}
- 14 **end**

Fig. 23 Pseudo code of projecting the ship's route

As the risk gradient changes, the result of the route projection varies as shown in Fig. 22. This case illustrates that the smaller Radius was applied, resulting in the route projection predicated on the steeper risk gradient. This route projection algorithm is also represented as the pseudo code in Fig. 23.

4.3.3 Route projection based on risk gradient

According to the result of the preliminary route's projection, an algorithm was proposed to select a combination of the derived reference points, consequently enabling analyses and plots of the feasible route options. To be specific, all the feasible options of the route plans could be deduced by combining the reference points of the preliminary route on the risk contour map. This concept was mathematically modeled as follows. In case that n reference points are identified from P_{dep} to P_{arr} ,

the selection of r points among the reference points as combination is defined by Equation 9,

$$selection_r = {}_n C_r \quad (9)$$

where $selection_r$ is the number of all available options of selecting r points among n reference points, and ${}_n C_r$ is the possible number of combinations (r points) among n points. If there are three reference points based on the risk gradient as shown in Fig. 22 (a), the possible cases of the route options by selecting two of them are expressed as ${}_3 C_2$. On the other hand, if there are five reference points based on the risk gradient as shown in Fig. 22 (b), the possible cases are different, despite samely selecting two of them, in that the result is ${}_5 C_2$. The former cases as ${}_3 C_2$ are represented as shown in Fig. 24.

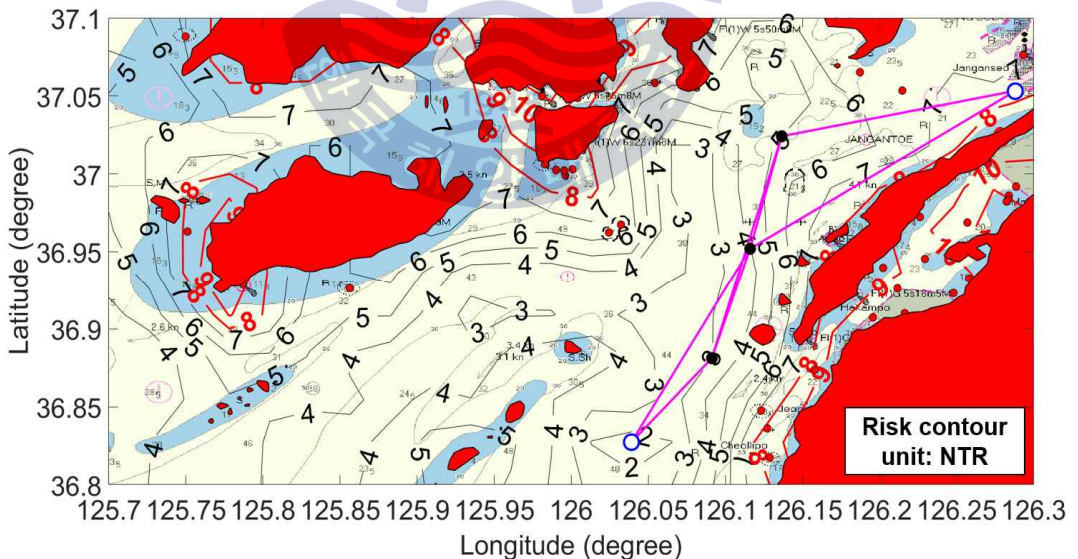


Fig. 24 Combination case as ${}_3 C_2$ among three derived reference points

Moreover, among all the identified reference points, the total possible cases of combination options are summarized by the binomial theorem (shown in Fig. 25) as described in Equation 10,

$$N(ALL) = {}_n C_0 + {}_n C_1 + {}_n C_2 + \dots + {}_n C_{n-1} + {}_n C_n = 2^n \quad (10)$$

where $N(ALL)$ is the total possible number of options from selecting none to selecting all, in the case of n reference points. For example, in case that there are three reference points in total, all cases of possible selections can be expressed as 8 cases (${}_3 C_0 + {}_3 C_1 + {}_3 C_2 + {}_3 C_3$).

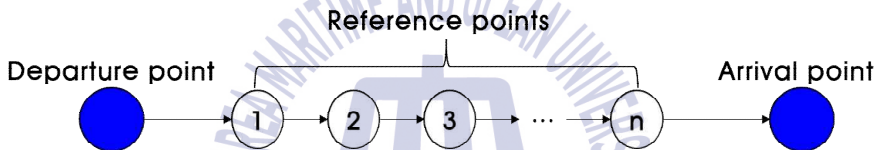


Fig. 25 Conceptual diagram of identified reference points between departure and arrival point for generalization of combination

Also, the analysis of applicability for the derived routes is carried out in order to exclude any routes touching the non-navigable areas in red color. Finally, except for the excluded route in this step, the feasible routes are confirmed and stored. Fig. 26 describe this process using pseudo code algorithm.

Furthermore, it was found that the reflected portion of each object in a specific route planning can be analyzed by a generalization of the suggested mathematical method. In other words, Fig. 27 illustrates the mathematical analysis of each object portion, which generalize the principle discovered by using Pascal's triangle.

Algorithm 3: Route planning selection

Read : refPoint, Non-navigable Area
Input : Gradient circle, departure position(P_{dep}), arrival position(P_{arr})
Output: all route plans with object set of $vector_Plan_{k,j}$

- 1 Mark k as label of all refPoints from P_{dep} to P_{arr}
- 2 Mark j as label of route when selecting j number of refPoints
- 3 Mark S as set of all refPoints
- 4 **for** $selection = 0$ to $Sizeof(S)$ **do**
- 5 | Plot line from P_{dep} to P_{arr} passing via $selection$
| Mark the line as $Plan_{k,j}$
- 6 | **for** $j = \min(j)$ to $\max(j)$ **do**
- 7 | | **if** $Plan_{k,j}$ enter Non-navigable Area **then**
- 8 | | | Define OBJ_{safe} as vertical integration per distance of $Plan_{k,j}$
| | | Define OBJ_{eff} as total distance of $Plan_{k,j}$
| | | Define OBJ_{conv} as number of waypoints on $Plan_{k,j}$
| | | Define $OBJ_{ability}$ as average risk gradient $Plan_{k,j}$
| | | Save $\{OBJ_{safe}, OBJ_{eff}, OBJ_{conv}, OBJ_{ability}\}$ as $vector_Plan_{k,j}$
- 9 | | **else**
- 10 | | | discard $Plan_{k,j}$ as not possible route
- 11 | **end**
- 12 **end**

Fig. 26 Pseudo code of route planning as per analysis of objects

For example, the routes located in the pink region stand for the cases that the reference points were not selected at all, thus connecting P_{dep} to P_{arr} straightforwardly. In this region of the route planning, the efficiency and convenience objects are reflected as the maximum portion, respectively, because of the direct lines. Nevertheless, the ability object is considered as the minimum portion, because there is no combination of the derived reference points as per the desired risk gradient. In contrast, the routes within the yellow region mean that the ability object is regarded as the maximum portion, as these routes combine all of the reference points identified by the inputted risk gradient.

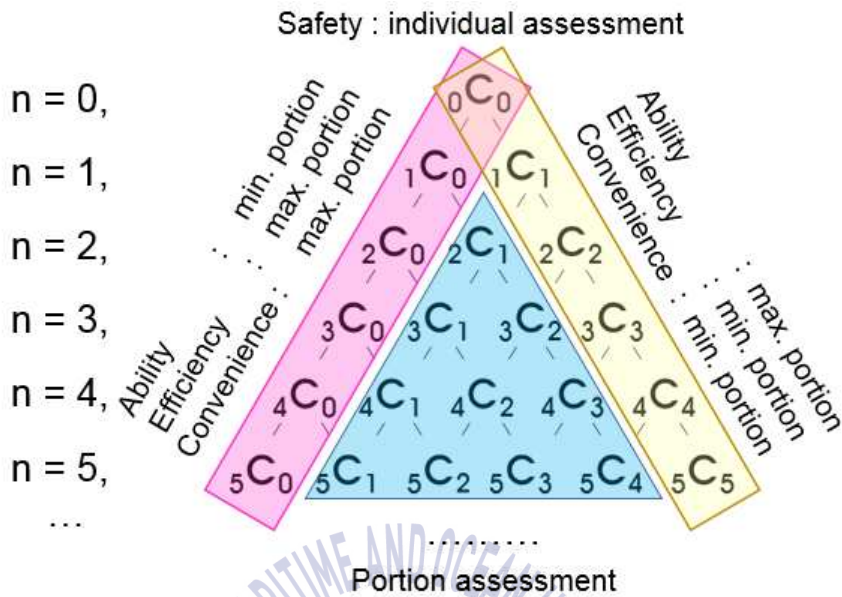


Fig. 27 Use of Pascal's triangle for generalization of analyzing portions of object in route planning algorithm

Particularly, these routes selecting all reference points are the most evasive route with the most number of waypoints as well as the longest distance among the possible cases on n row, thus making the portions of the efficiency and convenience objects least considered. In addition, the routes located in the blue region are cases where the portions of the three objects (efficiency, convenience, and ability) are distributed between the minimum and the maximum found in the pink and yellow region. Different from these three objects, the safety object scarcely has a general principle due to the irregular shape in the horizontal surface for the risk contour map on the ground that the safety object is measured by the cumulative risk per distance as suggested in Section 4.2.

4.3.4 Object-oriented route and smart navigation

As the last stage, the object-oriented routes are determined in comparison with the user's input with regard to each object. In other words, among the various feasible route options derived from the proposed technique, the routes that satisfy the preferences and intentions of the operators are finally found in order to realize smart navigation. This fit-for-purpose method is differentiated from the previous route planning which only focuses on optimization based on a specific algorithm especially connected with the efficiency. Hence, the route options are more flexible, relying on the situations. The proposed technique suggests routes without causing a navigational traffic accident, since the non-navigable areas including hazard factor were excluded for safe navigation. Therefore, the object-oriented route that best fits into the corresponding circumstances as per user's input of portions for four main objects can be achieved, as the proposed technique serves as an effective decision-making tool of the route planning.

Chapter 5. Simulation Result and Application

5.1 Experimental case study of numerical simulation

5.1.1 Overview of numerical simulation

Numerical simulation using the model of the ship based on the study area was conducted in order to verify and validate the propose route planning technique (Jeong *et al.*, 2018d). The primary purpose of the simulation was to observe whether or not the proposed technique actually derives a result of routes as per suggested algorithms, and to quantitatively analyze the derived routes. The design of the simulation was based on two conditions: one was carried out under the default condition, where there was effect of neither tide nor weather, while the other was performed under the changed condition, where the influence of both tide and weather existed.

As shown in Fig. 15, the level of the risk contour lines in the study area was likely to increase, as the ship approaches the destination. This tendency is attributable to the fact that the closer the ship's position is to the pilot station of Pyeongtaek, the more obstacles and the shallower water depths are to be encountered, as the normal phenomenon during the phase of a coastal navigation.

The experimental values for R during the simulation were applied to find the feasible route options which are dependent on $Grad$. To be

specific, the simulation utilized five values of R as of 3, 3.75, 4.5, 5.25, and 6 nautical miles, which are regularly distributed. In case that there is no resolution with regard to application of R , there might be infinite numbers of cases, since so many real numbers are available for R during the test in Section 4.3.2. In consequence, using the designated resolution of R during the simulation, total 153 route plans were plotted as the feasible route options, which finally determines the object-oriented routes.

5.1.2 Results of objected-oriented routes

After all feasible 153 routes were analyzed by the proposed technique, the quantitative assessment of the objects as per corresponding criteria in Section 4.3.2 was carried out. During this process, normalization was utilized in order to relatively compare the portions of the different objects based on the common standard system.

The result of object-oriented routes under the default condition is shown as solid lines in Fig. 29. In this example, the simulation turned out the extreme cases as the maximum portion per each object. The numerical details are suggested in Table 4 in order to support understanding the results more objectively. The safety-based route under default condition is the path along the valley of the risk contour map, when it comes to comparison with topography. This route can be expressed as the one that minimize the cumulative risk per distance among the proposed routes, thus considering the safety portion as maximum. Also, the efficiency-based route represents that it significantly reduces the distance of total legs, as the route relatively closely passes by the non-navigable area rather than other proposed routes. In addition, the convenience-based route shows the smallest number of

waypoints in order to minimize the course alteration along the suggested route. Last, the ability-based route stands for the lowest average risk gradient, which indicates that the required supports or other back-up resources are minimized. However, the ability-based route takes the longest route in that the most evasive option is selected owing to duly consideration of the gradual risk gradient.

Additionally, a further result was verified as the changed sea condition was applied to the proposed route planning technique. The data of the changed sea condition were received by nearby stations: Taeon tidal station and Taeon ocean data buoy. The data were composed of tidal data as well as marine meteorological data such as wind, current, and visibility. As for the simulation, a random datum at a certain date and time (1800 KST, 12th December 2017) was adopted to carry out simulation, of which a tidal height was 2.15 meters, a wind speed was 5.6 m/s, a current speed was 0.46 knots, and a visibility was 10 nautical miles. Also, the size of unit area based on position fixing interval was calculated by 6 min to 3 min, in order to check sensitivity and overall verification. Owing to this changed condition, Fig. 28 demonstrates that the risk contour has become differently assessed and visualized.

Since the proposed technique was applied into the newly visualized risk contour on ENC, validation was made to check the availability. The result of the object-oriented routes under the changing condition is shown as dashed lines in Fig. 29. Also, the numerical details are suggested in Table 5.

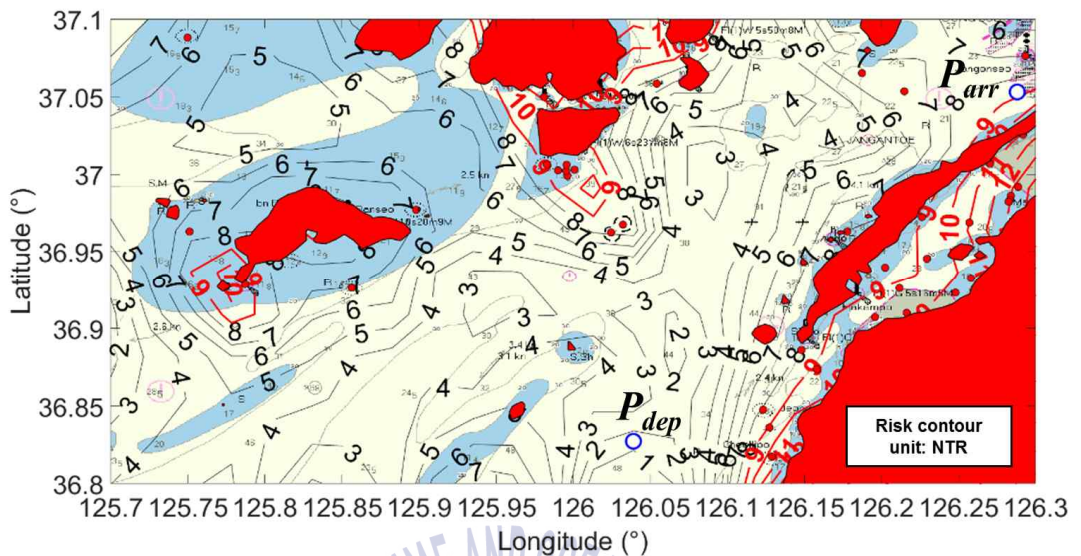


Fig. 28 Newly visualized risk contour map reflecting changed condition

The simulation results from both the default and changed condition indicates that the proposed route planning technique is available to be utilized for smart navigation in real-time under different conditions and environments. Also, even if the results were mainly based on the cases that makes each portion as a maximum, the operator can spontaneously select the portions of the objects, thus obtaining routes that reflect them. Therefore, this study has novelty in that it differs from the other previous studies that suggest a single optimized route with the use of efficiency-based algorithms.

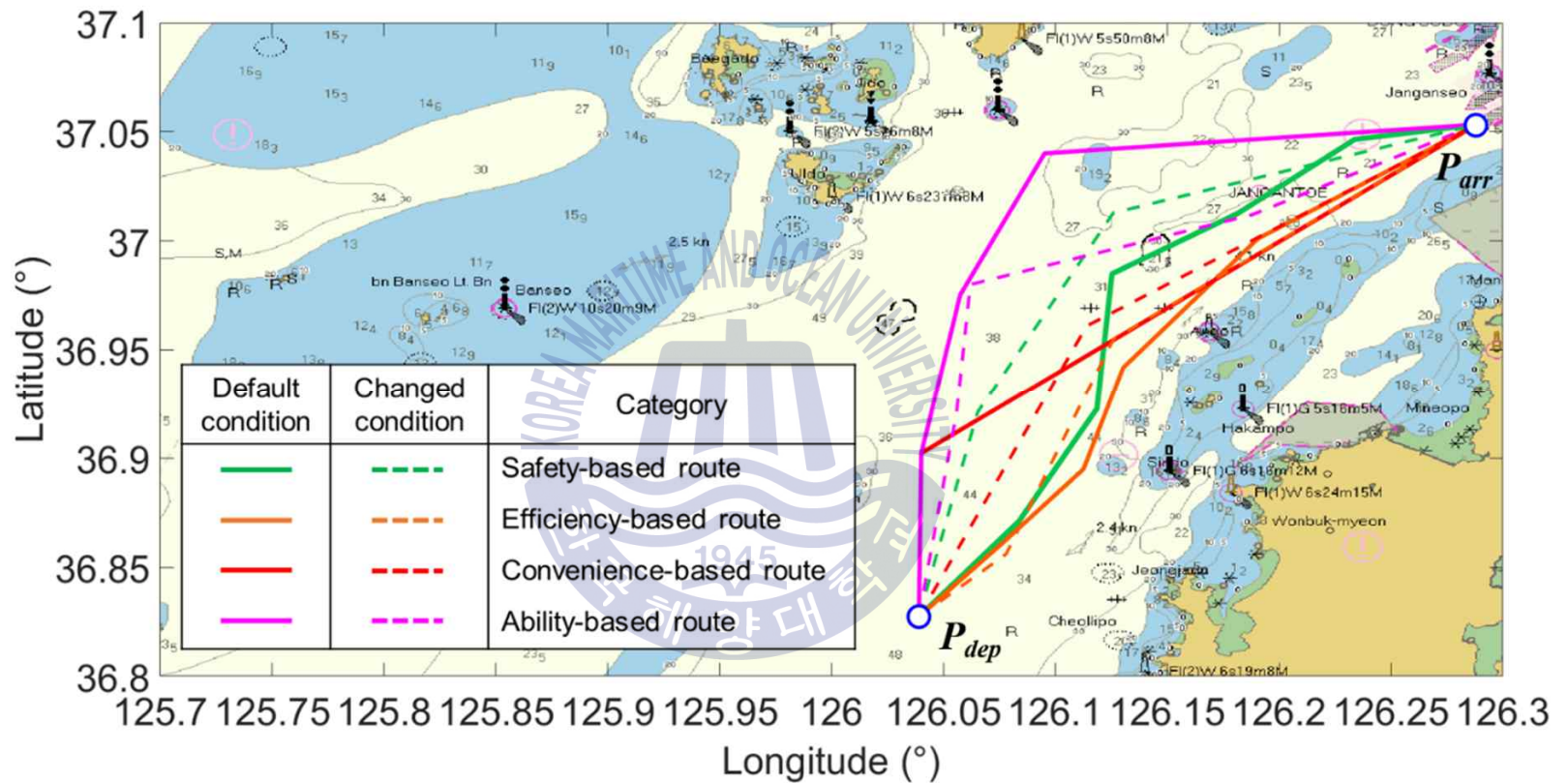


Fig. 29 Results of numerical simulations for object-oriented route planning as per each object made for maximized portion under the default condition (straight lines) and the changed condition of weather and tidal height (dashed lines)

Table 4 Result of the simulation for the object-oriented routes under the default condition

Role	Cumulative risk per distance [NTR]	Distance [NM]	Number of waypoints [EA]	Average risk gradient [NTR/NM]	Portion of safety [%]	Portion of efficiency [%]	Portion of convenience [%]	Portion of ability [%]
Safety-based route	4.6435	22.04	5	0.2829	42.58	38.12	Default	19.30
Efficiency-based route	5.4465	20.73	4	0.3009	3.70	76.09	16.05	4.14
Convenience-based route	5.2071	21.93	1	0.2843	12.35	33.46	38.96	15.23
Ability-based route	4.6609	25.12	3	0.2483	34.17	Default	18.81	47.03

Table 5 Result of the simulation for the object-oriented routes under the changed condition

Role	Cumulative risk per distance [NTR]	Distance [NM]	Number of waypoints [EA]	Average risk gradient [NTR/NM]	Portion of safety [%]	Portion of efficiency [%]	Portion of convenience [%]	Portion of ability [%]
Safety-based route	4.7196	22.49	3	0.3262	44.89	25.22	26.64	3.24
Efficiency-based route	5.9140	20.89	2	0.3511	3.92	57.95	38.13	Default
Convenience-based route	5.4099	21.03	1	0.3487	21.58	37.31	41.11	Default
Ability-based route	4.9790	23.58	3	0.3111	15.98	18.12	21.87	44.03

5.2 Application of object-oriented route technique

5.2.1 Evaluation of used routes

5.2.1.1 Structure of AIS data

The automatic identification system (AIS) is a tracking system of ship-specific data transmitted by transponders, which are utilized by both ships and shore stations such as vessel traffic services. The data of AIS are mainly comprised of three types, which are static data, dynamic data, and voyage data (International Maritime Organization, 2006; Liu and Chen, 2014; Zhang *et al.*, 2017). During this study, in order to apply the proposed technique for the purpose of evaluation of past tracks, statistical AIS data which were acquired from Korea Ministry of Oceans and Fisheries were analyzed.

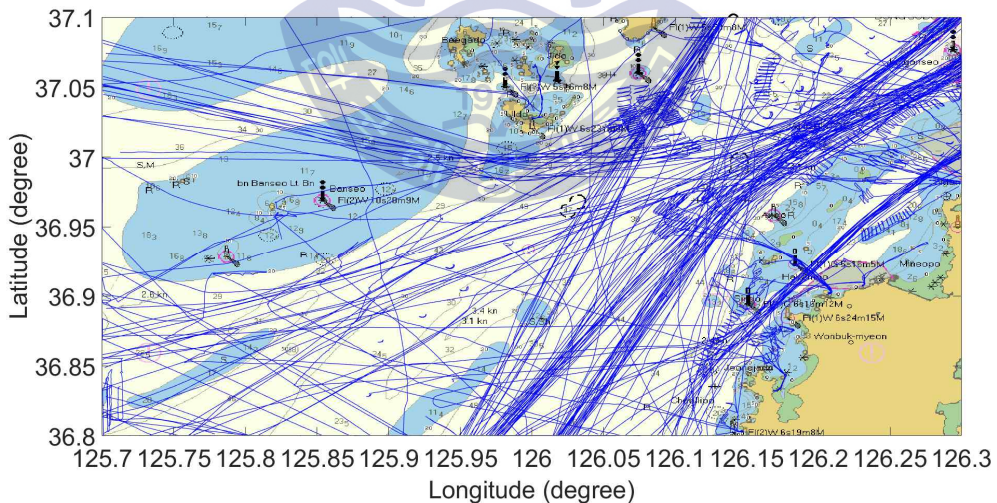


Fig. 30 Tracks of three-day AIS data from GICOMS database in the area

The total data within the experimental area for 3 months from September to December in 2017 were found to have 3,717 ships. These

AIS data for all ships in the region during three days, which are necessary for traffic analysis, were shown as blue lines in Fig. 30. During the preprocess of data, the outlier such as data with abnormal fluctuation were to be excluded. Then, the AIS data that match the model of the ships navigating from P_{dep} to P_{arr} within the experimental area were only extracted for the analysis. To be specific, the proposed technique filtered the static data that coincide with the ship's specifications, the dynamic data that coincide with those ships underway, and the voyage data that coincide with the ships entering Pyeongtaek LNG terminal, as shown in red lines in Fig. 31.

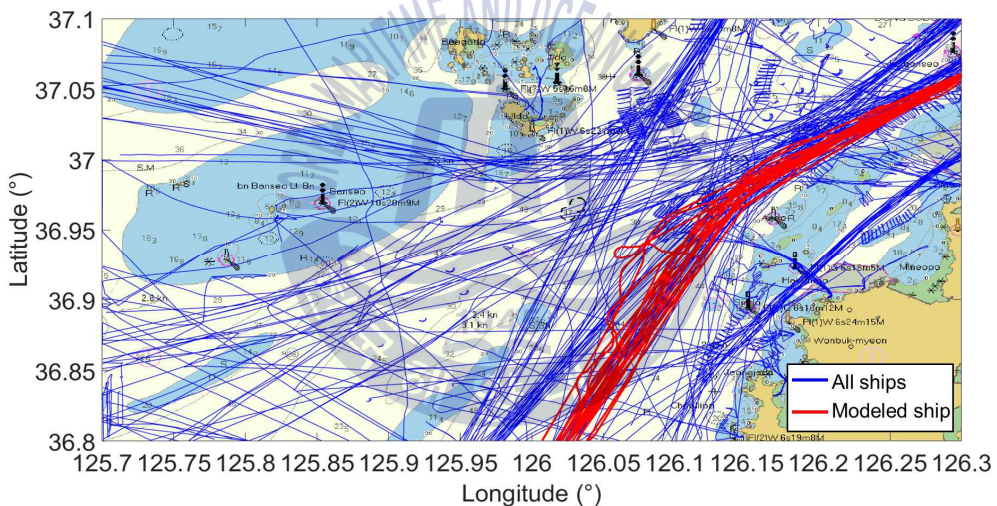


Fig. 31 Tracks of filtered AIS data matching the modeled ship and other conditions such as dynamic data and voyage data in the study area

In addition, external environments such as sea condition and tide heights were considered to be on the common standards as the default condition, so that the analysis and evaluation can be performed effectively. Nevertheless, the outlier such as extreme conditions including tropical warnings were also excluded because of the coherent application

to the route planning. As a result, total 36 statistical data that accurately match the model of the ships as well as the necessary direction of navigation were extracted; hence, these data were eventually identified in order to evaluate them through the proposed route planning technique.

5.2.1.2 AIS Data evaluation

Another case study of the proposed route planning technique was to evaluate the past track of statistical AIS data which had been accumulated from Section 5.2.1. Since the AIS tracks usually represent the continuous movements as curves instead of segmented lines for route plans, a boundary containing those tracks was firstly distinguished in the study area.

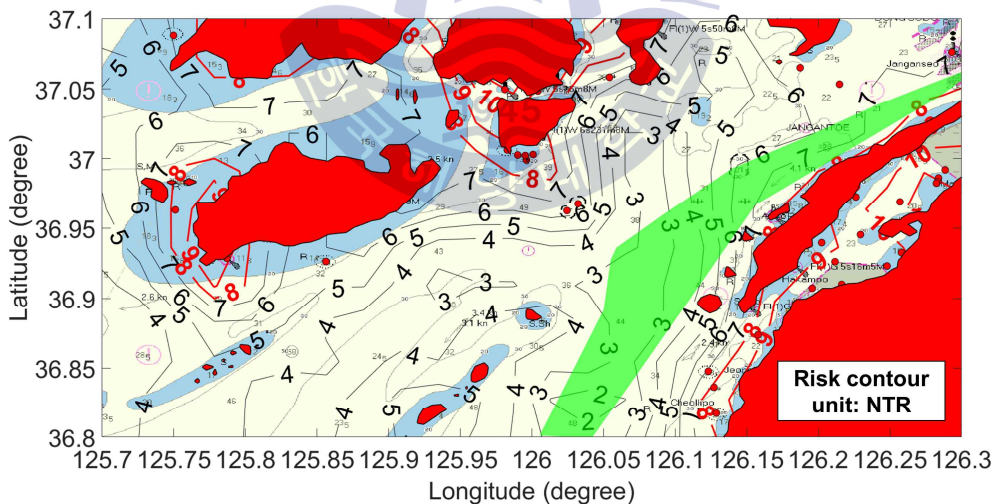


Fig. 32 Polygonal boundary of AIS tracks for evaluating the used routes

The polygonal boundary indicates the vertexes as connecting the outermost parts of the AIS tracks as illustrated in Fig. 32. Hence, the

routes that were derived by the proposed technique and came inside this boundary were the materials for the objective and quantitative evaluation. The evaluation was mainly two parts: to understand the actual route plans' tendency and to diagnose the portions of considered objects in actual routes.

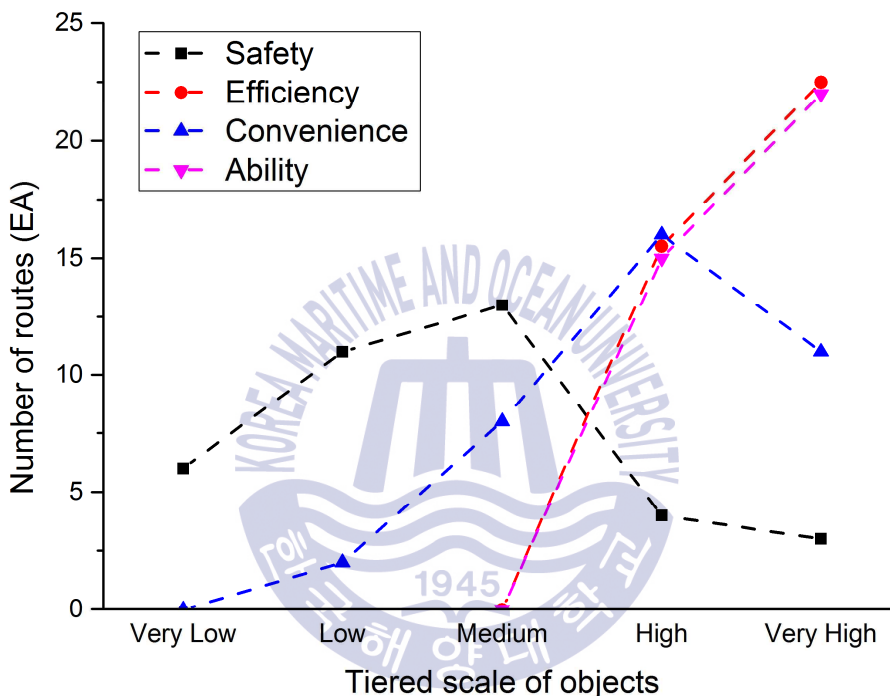


Fig. 33 Result of evaluation of the used routes by statistical AIS data according to a five-tier scale of each object

First, in order to understand the trends of the current routes, the analysis based on the five-tiered scale introduced in Section 4.2 was carried out. The result of the evaluation was represented as shown in Fig. 33. According to the analysis, it was found that the efficiency object showed relatively high scales as they mostly range between high and very high. This can be understood by the fact that most route plans focus on efficiency, i.e., the reduction of distance as a primary goal.

Similarly, the convenient object shows the distribution between medium and very high, which means that most of routes are based on the small number of waypoints from 1 to 3. As for the safety object, scales from very low to medium are most frequently observed. In other words, compared to the efficiency and convenience, the route planning follows the paths of which the safety is relatively weak, making the cumulative risk per distance high. Last, the ability object represents scales between high and very high. Nevertheless, owing to the inverse proportional relationship defined in Section 4.2, the result indicates that the average risk gradient is fairly high, requiring due attention, and supports to compensate for the necessary ability of navigation.

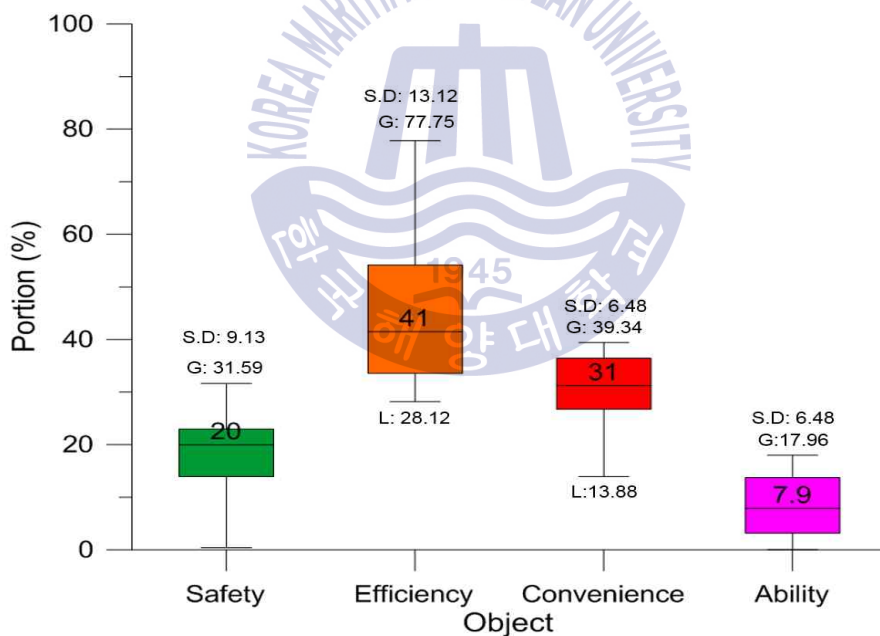


Fig. 34 Result of evaluation of the used routes by statistical AIS data according to reflected portions of each object (L: Lowest, G: Greatest, S.D: Standard Deviation)

Furthermore, as the second analysis, it is possible to evaluate the

portions of objects selected by the current vessels. Fig. 34 demonstrates the distribution of the object portions as a percent. These portions are evaluated by the relative comparisons among the derived routes within the polygonal boundary and normalization conducted in Section 5.1.2. The result indicates that the most considered object among the four elements is the efficiency. Then, the priorities of the portions were followed by the convenience, safety, ability. Specifically, the range of the efficiency object is between 28 % and 78 %, whereas the range of the ability of navigation is between default and 18 %. It can be summarized that the current routes do not have much attention on the rapid change of navigational traffic risk at the spatial area, which can be observed by the risk gradient on the visualized contour map.

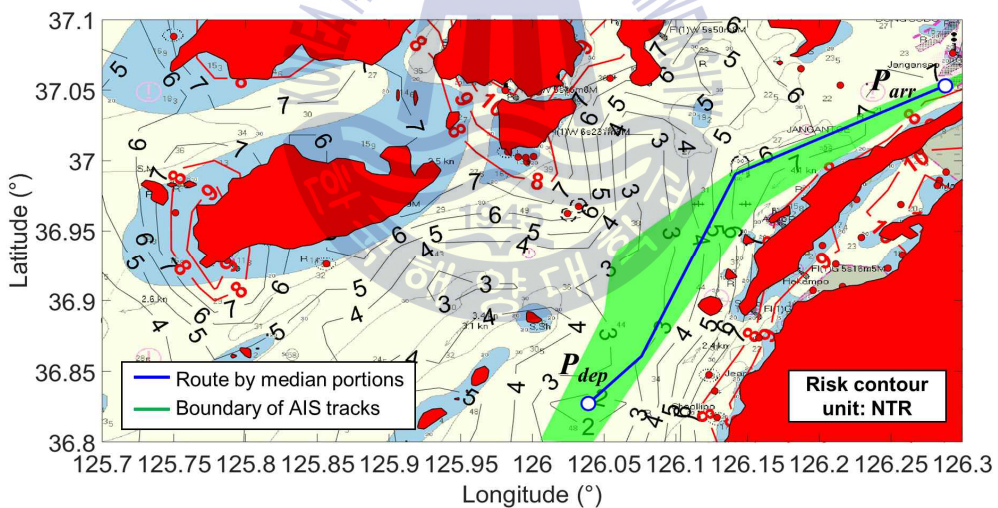


Fig. 35 Result of selecting each object's portion as median of AIS data

The evaluation of these portions means each object per an actual track can be quantitatively analyzed, thus making it possible for a user to select a certain route vice versa. In particular, among the evaluated portions of the routes, in case that an operator chooses a respective

portion for each object, a route reflecting the selected values can be extracted as a result. Fig. 35 shows the result of a route plan with the selection of each object as a median portion. This route is composed of each object as per 20% safety, 41% efficiency, 31% convenience, and 8% ability.

Consequently, the proposed technique for object-oriented route planning was validated as the effectiveness was confirmed by the two types of applicability based on AIS data: evaluation of the actual tracks of the current ships, and proposal of a new route plan selecting the portions of the analyzed AIS data's objects.

5.2.2 Analysis of navigational traffic accidents

Another verification of the proposed technique was conducted by application into the analysis of navigational traffic accidents (Jeong *et al.*, 2018b, 2018c). The scope of the accidents was circumscribed to ones that were defined in Section 2.4.1, which were caused by inappropriate management of routes.

5.2.2.1 Analysis of accident in Janganseong

Based on the survey of navigational traffic accidents within the experimental area and covered by Korea Maritime Safety Tribunal (2018b), a representative case as shown in Table 6 was identified and evaluated. The accident occurred while the ship headed to Gwangyang port after it departed from Pyeongtaek port. Now that data of sea conditions at that time were not available, they were obtained by

tracking of accumulated database by Taeon tidal station as shown in Fig. 36. Then, these raw data were utilized by the proposed technique in order to systematically analyze the navigational traffic accident in detail.

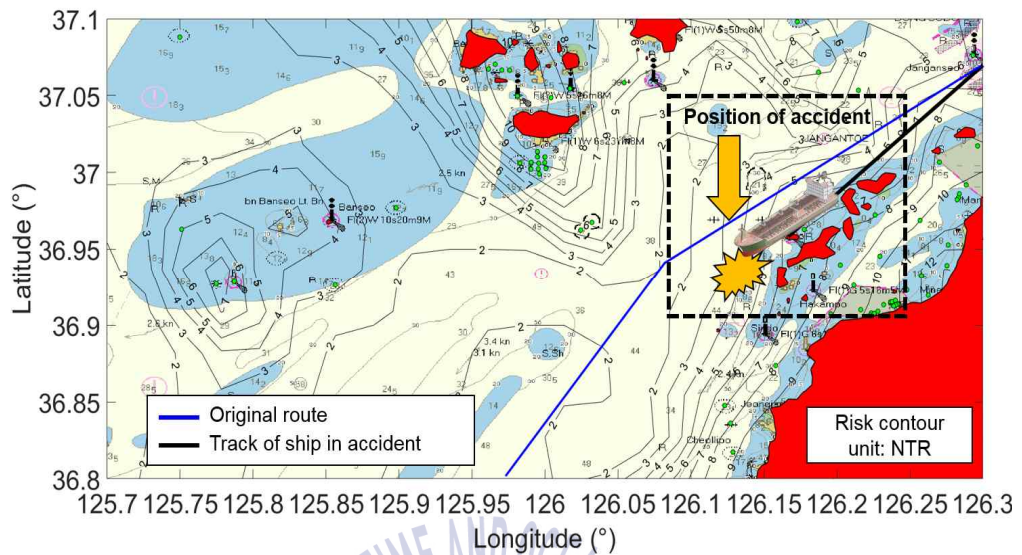
Table 6 Grounding accident of cargo ship SUN VIEW in study area

Accident Number	Busan tribunal 2012-021
Vessel name	SUN VIEW
Port of registry	Jeju, Korea
Ship's type	General cargo ship
Gross tonnage	4,205 GT
Engine type/output	Diesel engine/2,059KW
Length/Breadth	98m/18m
Time and Date	0135LT, 12th Oct. 2011
Proceeding speed	9 knots
Position	Latitude: 36° 57' 30'' N Longitude: 126° 10' 00'' E (Nearby the west end of Ando)
Sea condition	Tidal height: 3.04 m Wind speed: 0.3 knots Current speed: 2.05 knots Visibility: 6 NM
Description	After keeping steady on 224 degrees when it passed by a waypoint nearby Janganseo, the ship ran aground without proper alteration of the course.
Details of causes in report	1) Officer's negligence on watch: Second mate fell asleep during the watch, resulting in deviation from the original route 2) Inappropriate management of navigational watch During nighttime, the watch was operated by an officer without a quartermaster.

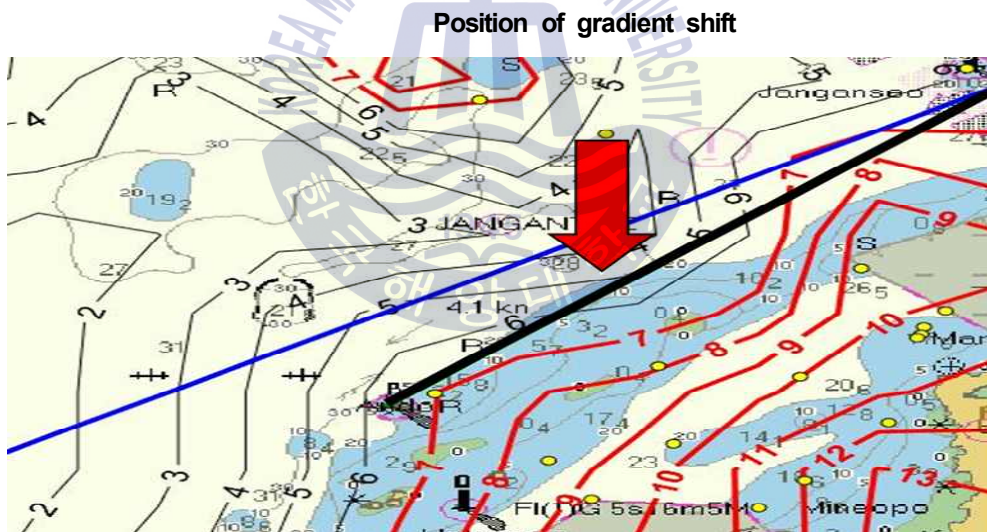


Fig. 36 Sea condition data received from Taean tidal station





(a) overview of accident situation in study area



(b) Zoomed-in view of accident route for indicating position of gradient shift

Fig. 37 Charted diagram of both original and accident route on the risk contour visualized by reflection of the ship's data in accident:

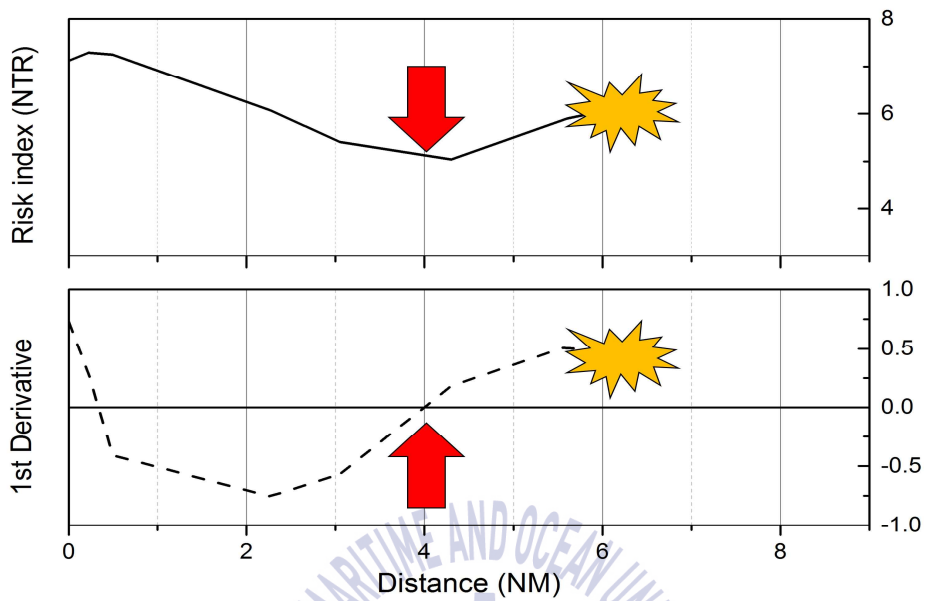
The plotting of both the originally normal course and the track of the ship involved in the accident was carried out as shown in Fig. 37 (a). In order to illustrate the accident in more detail, the accident area was zoomed in as shown in Fig. 37 (b). The red arrow stands for the unexpected shift of the risk gradient on the risk contour map, which was supposed to be gradually decreasing along the normal route.

According to the analysis by the proposed technique, the results were demonstrated as shown in Fig. 38. The above graph along the distance in Fig. 38 (a) shows that the risk index unexpectedly increased at the marked point as the ship enters the area which had not been planned. Specifically, the below graph in Fig. 38 (a) as the first derivative made it possible to discern the point of the risk gradient (at a distance of 4 NM) intuitively as the value, the slope at the point, changes from the negative (decreasing) to positive (increasing) by passing through 0. These results show a discrepancy with the results of the normal route as shown in Fig. 38 (b). In other words, the risk index was supposed to decline as the ship headed out to open sea, as the above graph in Fig. 38 (b). Also, this could be understood by the negative value of the first derivative prior to distance of 6 NM as shown in the below graph of Fig. 38 (b).

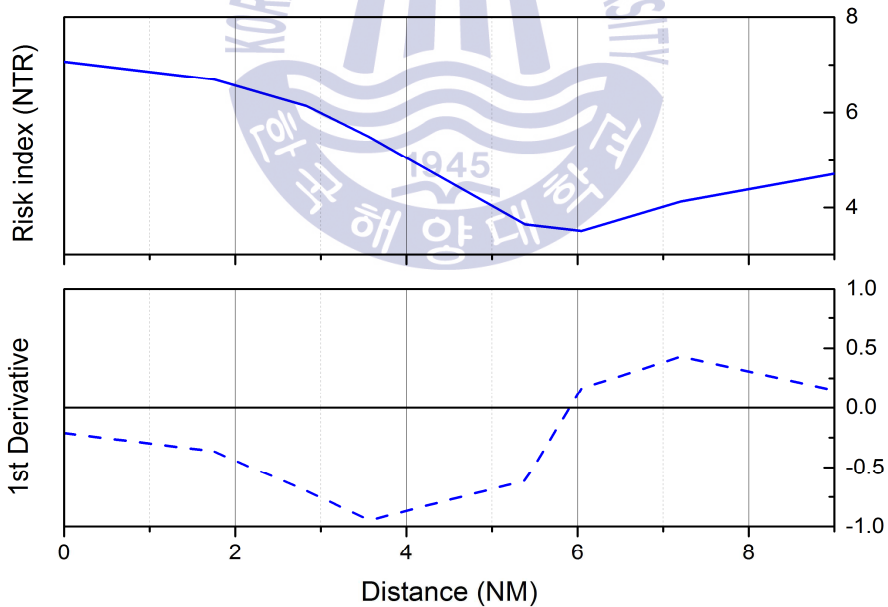
Furthermore, using the proposed technique enables the users to find out the causes of the accident as shown in Fig. 39. In this example, the causes of the accident was interrelated with the safety and ability object. First of all, there was the unexpected shift of 1st derivative of the risk gradient from negative to positive, as the ship diverted from the original course. Second, in order to handle the abrupt change of this risk gradient, there was no sufficient supports such as a quartermaster on watch. If the designated quartermaster of the watch had been on the

wheelhouse, the accident might have been probably prevented. Last, as the ship entered the region which the route plan did not aim for, there was an excessive risk value (cumulative) per distance, which is related to the measurement of the safety object. Within this area having excessive risk per distance, mishandling of the ship eventually led to the accident.





(a) case of the ship's route in accident



(b) case of the ship's route in original plan

Fig. 38 Comparison of navigational traffic risk along distance and its first derivative

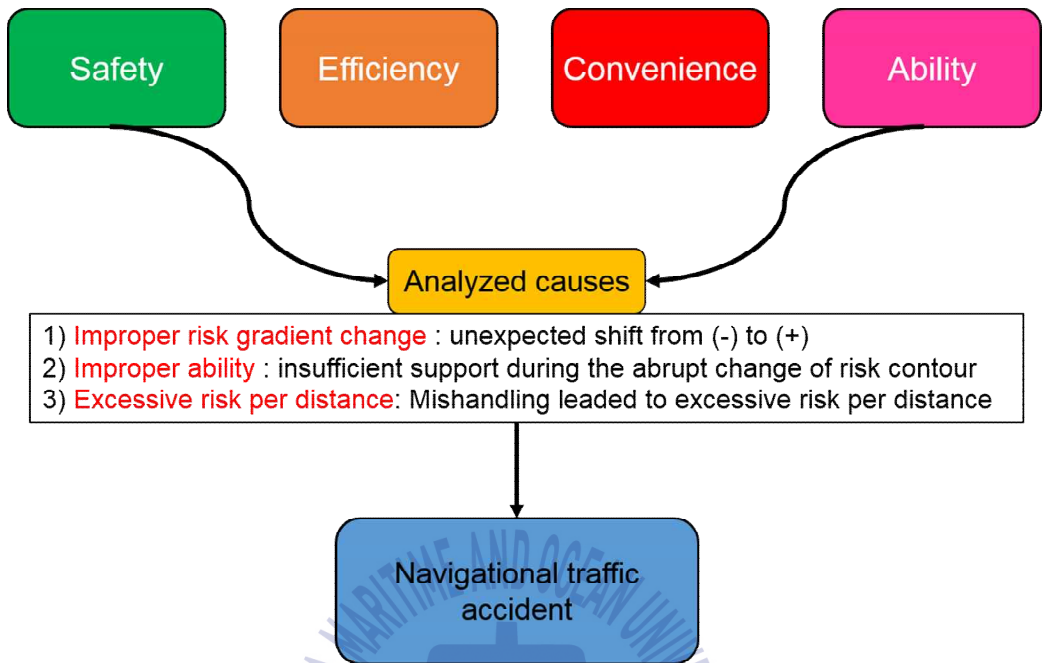


Fig. 39 Analysis of the navigational traffic accident to find out causes according to involved objects in the given case study

In sum, the application of the object-oriented route planning helps causes of navigational traffic accidents to be identified and analyzed in a more quantitative and objective manner. This result indicates that the proposed technique is beneficial as it utilizes the systematic methods in comparison with the a qualitative investigation conducted in tribunals. Furthermore, not only can it identify and analyze the causes after an accident occurs, but also the proposed technique can anticipate the likelihood of an accident prior to the occurrence, since it is available to connect this method with pre-warning or pre-alarm to operators. Thus, this technique has ultimate advantages in terms of applicability to navigational traffic accidents both beforehand and afterwards.

5.2.2.2 Analysis of accident in New Zealand Coast

In order to validate the application to analyzing navigational traffic accidents other than the study area, the additional case study was conducted in Bay of Plenty in New Zealand (TIAC, 2014). The details of the accidents are given in Table 7, which was one of the most typical cases for accidents resulting from inappropriate routes.

Table 7 Grounding accident of container ship RENA in another area

Accident Number	Marine inquiry 11-204
Vessel name	RENA
Port of registry	Jeju, Korea
Ship's type	Container ship
Gross tonnage	37,209 GT
Engine type/output	Diesel engine / 21,680KW
Length/Breadth	224.5 m / 32.2 m
Time and Date	0214LT, 5 th Oct. 2011
Proceeding speed	18 knots
Position	Latitude: 37° 32' 24" S Longitude: 176° 25' 42" E (Astrolabe Reef)
Sea condition	Tidal height: 1.79 m Wind speed: 15 knots Current speed: 0.5 knots Visibility: 10 NM
Description	While heading to Tauranga pilot station, the ship ran aground on Astrolabe with full speed.
Details of causes in report	1) Officer's negligence on watch: Second Mate did not pay attention to the navigational circumstances despite the ship's operation in risk area 2) Inappropriate change of route In order to make time of arrival, Second Mate kept changing course close to the shoreside

Fig. 40 shows the application of the technique into analysis of this accident. In this case, raw data for bathymetry were procured from the National Institute of Water and Atmospheric Research in New Zealand. Since the Second Mate adjust the course in order to reduce the two miles from Aristolabe reef to one mile to save time, he unexpectedly encountered the increase of the route risk, thus making the ship aground.

Looking into more details with the use of a graph (shown in Fig. 41) for investigation, the risk index was supposed to start to increase at 5 NM distance. However, after the route was changed, the ship experienced that increase right after passing almost 2 NM distance. Moreover, the risk gradient on the risk contour map was also found to be a positive value at the unexpected position, due to the ship's approach to Astrolabe reef.

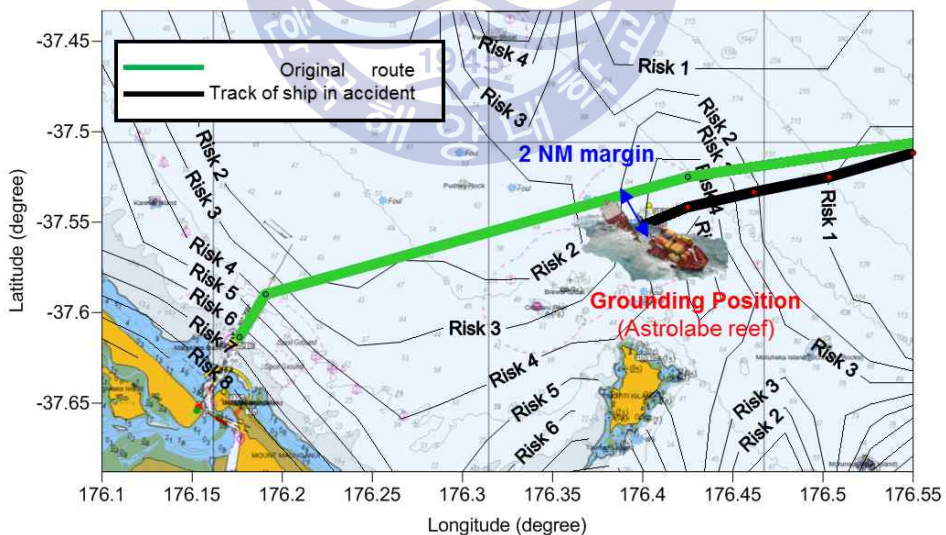


Fig. 40 Charted diagram of both original and accident route on the risk contour visualized by the ship's data in accident (New Zealand)

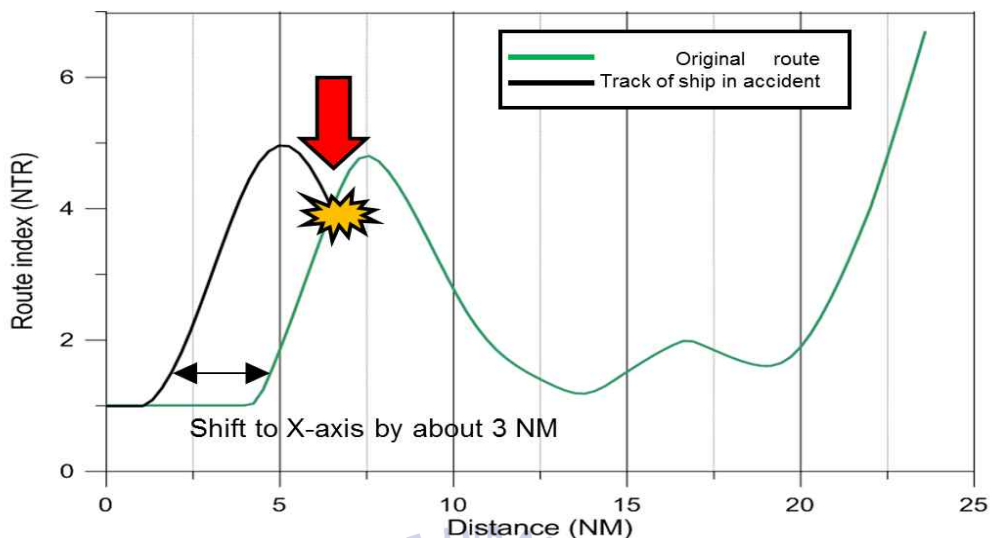


Fig. 41 Analysis of navigational traffic accident using graphical method

Therefore, the result of analysis indicates that the ship should have been operated carefully with sufficient ability of navigation within this area due to the abrupt change of risk index. For instance, as the ship approaches the coastal area prior to arrival at the pilot station, the master's operation as well as back-up assistance from additional watchkeepers was mandatory. The accident report was consistent with the analysis of the accident in that even if the master was on the bridge, there was no additional support by the officer. Also, the officer should have known the result of the improper route planning. However, he was negligent on the adjusted course in terms of entering the risky area, which causing the ship to be grounded.

In conclusion, the navigational traffic accidents can be investigated by application of the object-oriented route technique no matter where the accidents were. Furthermore, it is expected that this technique could be utilized for the purpose of preventative measures such as warning to the navigators.

5.3 Integration on ECDIS for training

The proposed technique in this study was further applied to integration on ECDIS for the sake of training operators (shown in Fig. 42). Now that ENC data in ECDIS are composite of individual cells, the new concept of integrating the developed mapping tools was introduced: 3D-based map from Google Earth (Google Earth, 2018), Risk contour map, and Electronic Navigation Chart (Jeong *et al.*, 2018c).

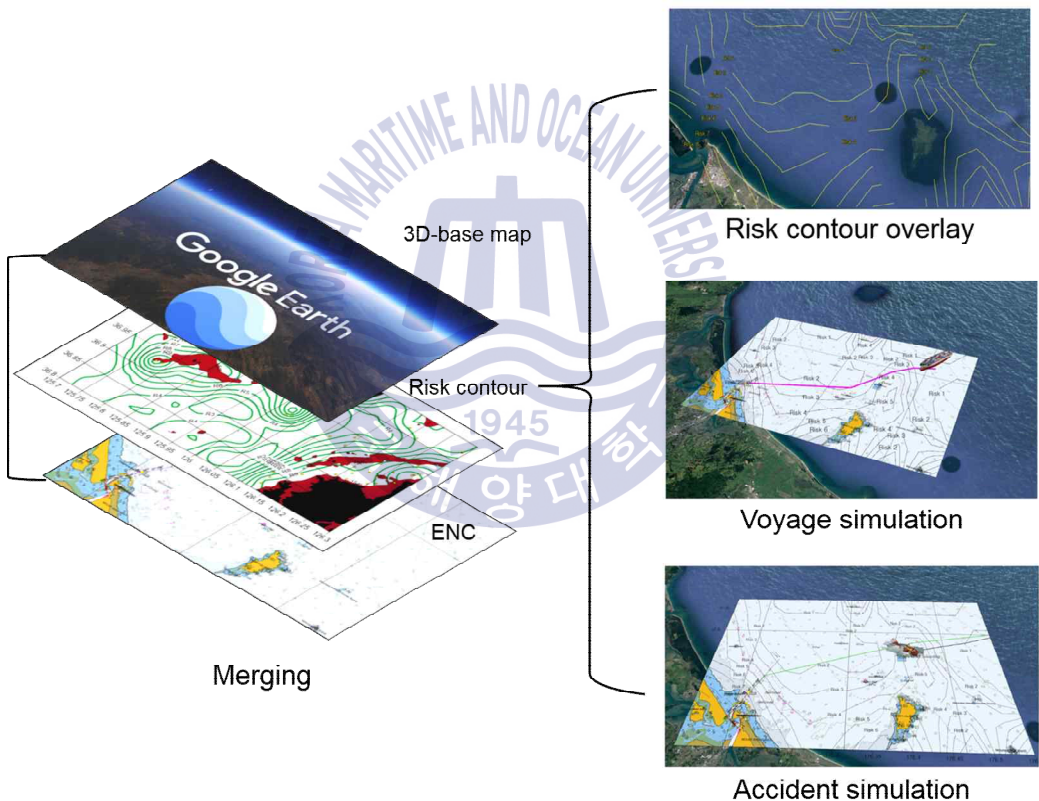


Fig. 42 Integration on ECDIS using 3D-based training and simulation materials

The modeled technique demonstrates that the risk contour map was overlaid on 3D terrestrial map by enabling the operators to more easily

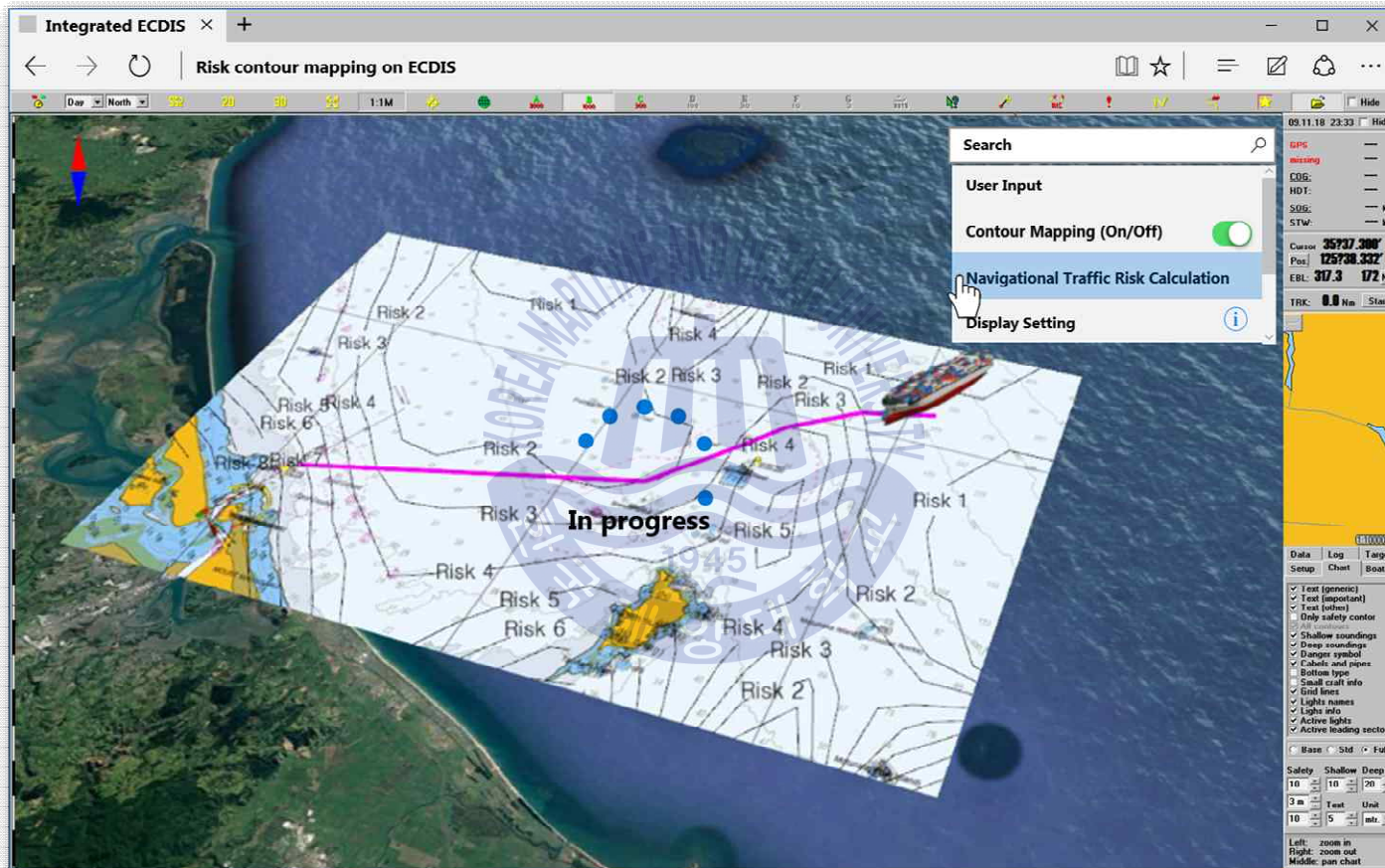


Fig. 43 Mock-up design of integrated Google map and risk contour map on ECDIS

understand the corresponding circumstances with the help of visualizing the real feature of the navigable area. Also, a simulation of the object-oriented route planning can be conducted by utilizing both 2D-based ENC and 3D-based map as shown in Fig. 43. This simulation would support better decision-making on routes because of comprehensive viewpoint to the expected navigation. Finally, a simulation of a navigational traffic accident could enhance the operators' cognitive ability in order to be vigilant at situational awareness. Therefore, using this technique as integration on ECDIS, the visual-aid in addition to other sensory elements can support the decision-making on planning a route in maritime navigation.

5.4 Discussion

In this study, the object-oriented route planning technique is based on four main objects as the safety, efficiency, convenience and ability of navigation. In order to provide operators with options to choose for the intended weight of each object, the proposed technique enables quantitative selections as per their purposes, which is termed as smart navigation. Therefore, the study is differentiated from previous studies that only focus on an efficiency-based route as an optimal option. However, this study can be further improved after the technique of automatic selection of the objects to be considered.

Moreover, the proposed technique was tested in the coastal regions of Korea and New Zealand. However, in case that a risk contour mapping seems too abnormal or extreme, the proposed technique is difficult to be applied, in addition to the some cases that the intended direction of navigation has limitations of application on the risk contour map, i.e., when following the direction of the contour line. In order to broaden

and generalize its application, regardless of areas, the technique should be further extended to other testing areas and scopes such as ocean navigation.

On top of that, since this paper was focused on the path planning based on stationary objects related to the navigational traffic risks at the appraisal and planning stage, it is necessary to develop an enhanced technique with algorithms, which include obstacle and collision avoidance as well as route follow-up. In particular, data analysis of dynamic risk factors should be integrated with the risk contour mapping to execute automated navigation. Therefore, operators can recognize and determine the situation, and react to the dynamic environment. In other words, dynamic factors should be considered in order that the proposed technique can be extended to the execution and monitoring stage. Hence, this research would compose an important module of marine robotics that has applicability to the next generation's autonomous cargo ships, underwater vehicles, and land vehicles, without restrictions on sizes.

Even if the aforementioned matters should be dealt with for improvement, the proposed technique has advantages in that it quantified the navigational traffic risks, visualized the risk contour mapping as a continuous method, and suggested the object-oriented routes for smart navigation in the corresponding circumstances by the operators. As verified by the result of applications, the proposed technique will have the possibility of extension of the application in various areas. Therefore, not only extant ship, but also future autonomous vehicles will be operated with the help of better decision-making approaches.

Chapter 6. Conclusion and future work

In this study, an object-oriented route planning technique was proposed. The proposed technique was intended to help operators to objectively plan fit-for-purpose routes for smart navigation in accordance with changing situations as well as different preferences. First, as the framework of the proposed route planning technique, risk contour mapping was developed. In order to visualize the risk contour map, factors influencing navigational traffic risk, i.e., absolute danger, hazard factor, and influential factor were structured and assessed. Based on the quantified navigational traffic risk index, the contour map was expressed in the connected curves on the navigable area. Next, as the fundamental part, the object-oriented route planning technique was suggested. The four main objects as the safety, efficiency, convenience, and ability of navigation were defined and measured by criteria such as cumulative risk per distance, total distance of the legs, total number of waypoints, and average risk gradient. The proposed technique utilizes the contour-based route projection model as per intended risk gradient, combines reference points, and generalizes regular tendency among the selected routes accordingly.

To verify the proposed technique and its effectiveness, experimental case study of numerical simulation, evaluation of used routes, and analysis of navigational traffic accidents was conducted. The results of the numerical simulation in the study area demonstrate that operators

can plan the ship's route adaptively by adjusting the portions of the objects. As examples, object-oriented routes in case of making the respective object's portion maximized were compared not only in the default condition of the external environments, but also in the changing conditions in real-time. In addition, by analyzing the statistical AIS data in the study area, the used routes by navigators were evaluated in terms of the tendency of considered objects. The evaluation includes the five-tier scale of the corresponding objects as well as reflected portions by relative comparisons. Furthermore, the other case study was to analyze causes of navigational traffic accidents. To do this, the accident cases not only in the study area, but also in New Zealand as additional validation was scrutinized in that they were typical accidents resulting from inappropriate route selections. The proposed technique showed that it is possible to identify and analyze the objects involved in the accidents in a systematic manner. The last application for the suggestion was to develop 3D-based training program that integrates ENC with the risk contour mapping as a cell. The newly integrated ECDIS is expected to serve as an important role in simulating maritime navigation focusing on the optimized routes prior to executing a voyage.

Nevertheless, other factors such as sea conditions in more details, dynamic objects or moving ships should be reflected in the further study in order to develop this study as a component module of the automated navigation process even during the execution and monitoring phases. Specifically, based on this study focusing on the route planning based on stationary objects before execution, further study will develop an enhanced technique with new algorithms, which include obstacle and collision avoidance as well as route follow-up. In other words, the future study will integrate data analysis of dynamic risk factors with the risk

contour mapping to execute automated navigation. As a result, vehicles will be able to recognize and determine the situation, and autonomously react to the dynamic environments. Then, the improved automated method can be a significant contribution to the fully autonomous navigation, which specializes in maritime robotics in the future. Finally, more in-depth studies connected with the improvement of the proposed risk contour mapping should be considered because of the wide applicability.



References

- Andersson, A. (2015) Multi-objective optimisation of ship routes, Chalmers University of Technology.
- Bialystocki, N. and Konovessis, D. (2016) ‘On the estimation of ship ’ s fuel consumption and speed curve : A statistical approach’ , *Journal of Ocean Engineering and Science*. Elsevier B.V., 1(2), pp. 157-166. doi: 10.1016/j.joes.2016.02.001.
- Barrass, C.B. (2004) ‘Thirty-Two Years of Research into Ship Squat’ , Squat Workshop 2004, Elsfleth/Oldenbourg, Germany.
- Bijlsma, S. J. (2001) ‘A Computational Method for the Solution of’ , *Navigation, Journal of the Institute of Navigation*, 48(3), pp. 145-154.
- Bijlsma, S. J. (2002) ‘On the applications of optimal control theory and dynamic programming in ship routing’ , *Navigation, Journal of the Institute of Navigation*, 49(2), pp. 71-80.
- Bijlsma, S. J. (2004) ‘On the applications of the principle of optimal evolution in ship routing’ , *Navigation, Journal of the Institute of Navigation*, 51(2), pp. 93-100. doi: 10.1002/j.2161-4296.2004.tb00343.x.
- Casola, J. H. and Wallace, J. M. (2007) ‘Identifying weather regimes in the wintertime 500-hPa geopotential height field for the Pacific-North American sector using a limited-contour clustering technique’ , *Journal of Applied Meteorology and Climatology*, 46(10), pp. 1619-1630. doi: 10.1175/JAM2564.1.
- Chen, J. J. *et al.* (2014) ‘Liver hydatid CT image segmentation based on localizing region active contours and modified parametric active contours’ ,

Proceedings - 2014 7th International Conference on BioMedical Engineering and Informatics, BMEI 2014, (Bmei), pp. 217-221. doi: 10.1109/BMEI.2014.7002773.

Chen, J., Qiao, C. and Zhao, R. (2004) 'A Voronoi interior adjacency-based approach for generating a contour tree', *Computers and Geosciences*, 30(4), pp. 355-367. doi: 10.1016/j.cageo.2003.06.001.

Chin, H. C. and Debnath, A. K. (2009) 'Modeling perceived collision risk in port water navigation', *Safety Science*. Elsevier Ltd, 47(10), pp. 1410-1416. doi: 10.1016/j.ssci.2009.04.004.

Korea Gas Corporation. (2009a) *Port Information and Terminal Regulations - Incheon*.

Korea Gas Corporation. (2009b) *Port Information and Terminal Regulations - Pyeongtaek*.

Cronin, T. (1995) 'Automated reasoning with contour maps', *Computers and Geosciences*, 21(5), pp. 609-618. doi: 10.1016/0098-3004(94)00100-9.

Danilo, C. and Melgani, F. (2016) 'Wave Period and Coastal Bathymetry Using Wave Propagation on Optical Images', *IEEE Transactions on Geoscience and Remote Sensing*, 54(11), pp. 6307-6319. doi: 10.1109/TGRS.2016.2579266.

Eniram, 2018. Eniram ROUTE, <https://www.eniram.fi/services/route/>. (Accessed 08 Aug 2018).

Equasis (2016) 'The world merchant fleet in 2016 Statistics from Equasis', pp. 1-64. doi: 10.1109/CECNET.2011.5768157.

Goerlandt, F. *et al.* (2015) 'A risk-informed ship collision alert system: Framework and application', *Safety Science*. Elsevier Ltd, 77, pp. 182-204. doi: 10.1016/j.ssci.2015.03.015.

Google Earth (2018) Google Earth Map, <https://www.google.co.kr/intl/ko/earth/> (Accessed 10 Oct 2018).

Gu, H. *et al.* (2015) 'Automatic contour-based road network design for

optimized wind farm micrositing’ , *IEEE Transactions on Sustainable Energy*, 6(1), pp. 281–289. doi: 10.1109/TSTE.2014.2369432.

Guinness, R. E. *et al.* (2014) ‘A method for ice-aware maritime route optimization’ , *Record - IEEE PLANS, Position Location and Navigation Symposium*, pp. 1371–1378. doi: 10.1109/PLANS.2014.6851512.

Hetherington, C., Flin, R. and Mearns, K. (2006) ‘Safety in shipping: The human element’ , *Journal of Safety Research*, 37(4), pp. 401–411. doi: 10.1016/j.jsr.2006.04.007.

Hoburg, J. F. (2004) ‘Modeling Maglev Passenger Compartment Static Magnetic Fields From Linear Halbach Permanent-Magnet Arrays’ , *IEEE Transactions on Magnetics*, 40(1 D), pp. 59–64. doi: 10.1109/TMAG.2003.821559.

Hyundai Merchant Marine (2018), *Operation Guidance*, PO-MC-102-008, ECDIS Basic Operation Guidance.

International Association of Lighthouse Authorities (2018) *Navguide 2018*. ST Germain En Laye.

International Association of Marine Aids to Navigation and Lighthouse Authorities (2009) *IALA Risk Management Tool for Ports and Restricted Waterways*, *International Association of Marine Aids to Navigation and Lighthouse Authorities*. doi: 10.1016/j.ress.2010.01.009.

International Maritime Organization (2001) *Revised Maritime Policy and Requirements for a Future GNSS*.

International Maritime Organization (2002a) *Guidelines for Formal Safety Assessment (FSA) for Use in the IMO Rule-making Process*, *International Maritime Organization*. doi: 10.1163/092735209X12499043518304.

International Maritime Organization (2002b) *Safety of Life at Sea - Safety of Navigation Chapter V, SOLAS Convention*.

International Maritime Organization (2006). Model Course 1.34 Automatic Identification Systems.

International Maritime Organization (2008) *Adoption of the Code of the International Standards and Recommended Practices for a Safety Investigation into a Marine Casualty or Marine Incident, Resolution MSC.255(84)*.

Javanmardi, J. *et al.* (2006) 'Feasibility of transporting LNG from South-Pars gas field to potential markets' , *Applied Thermal Engineering*, 26(16), pp. 1812-1819. doi: 10.1016/j.applthermaleng.2006.02.003.

Jebsen, J. J. and Papakonstantinou, V. C. (1997) *Evaluation of the Physical Risk of Ship Grounding*. Massachusetts Institute of Technology.

Jeon, H. (2018) *Development and Application of Collision Risk Assessment System for establishing Optimum Safe Route*. Korea Maritime and Ocean University.

Jeong, M., Lee, M. and Lee, E. (2017) 'A Study on the Visualization of HNS Hazard Levels to Prevent Accidents at Sea in Real-Time' , *Journal of the Korean Society of Marine Environment & Safety*, 23(3), pp. 242-249.

Jeong, M., Lee, M. and Lee, E. (2018a) 'A Study on Intuitive Technique of Risk Assessment for Route of Ships Transporting Hazardous and Noxious Substances' , *Journal of Navigation and Port Research*, 42(2), pp. 97-106.

Jeong, M., Lee, E., and Lee, M. (2018b) 'An Adaptive Route Plan Technique with Risk Contour for Autonomous Navigation of Surface Vehicles' , *Proceedings of MTS/IEEE, OCEANS, 2018 - Charleston*.

Jeong, M., Lee, E., and Lee, M (2018c) 'A Purpose-Oriented Technique for Route Planning of Ships based on the Concept of Risk Isoline Curves' , *Proceedings of International Association of Institutes of Navigation World Congress (IAIN) 2018*.

Jeong, M., Lee, E., Lee, M and Jung, J. (2018d) 'Multi-criteria Route Planning with Risk Contour Map for Smart Navigation' , *Ocean Engineering*, 172(2019), p. 72-85.

Kang, D. *et al.* (2015) 'Automatic Route Checking Method Using Post-

processing for the Measured Water Depth’ , *Proceedings of International Association of Institutes of Navigation World Congress 2015*, pp. 20–23.

Kanungo, T. *et al.* (2002) ‘An Efficient k -Means Clustering Algorithm : Analysis and Implementation’ , *IEEE Transactions on Pattern Analysis and Machine Intelligence*, 24(7), pp. 881–892.

Kim, C. and Lee, H. (2012) ‘A Basic Study on Assessment Criterion of the Risk Factor for the Marine Traffic Environment’ , *Journal of the Korean Society of Marine Environment & Safety*, 18(5), pp. 431–438.

Kobayashi, E., Asajima, T. and Sueyoshi, N. (2011) ‘Advanced Navigation Route Optimization for an Oceangoing Vessel’ , *TransNav, the International Journal on Marine Navigation and Safety of Sea Transportation*, 5(3), pp. 377–383.

Korea Hydrographic and Oceanographic Administration (2018). West Coast of Korea Pilot (2018 Edition)

Korea Coast Guard (2014), Korea Coast Guard 2014 White Paper

Korea Maritime Safety Tribunal (2018a).

<https://www.kmst.go.kr/kcom/cnt/selectContentsPage.do?cntId=21010000> (Accessed 16 August 2018).

Korea Maritime Safety Tribunal (2018b). Accident Position Information Based on Electronic Chart. http://www.kmst.go.kr/WebVMS_KMST/WebVMS.jsp. (Accessed 30 August 2018).

Kristiansen, S. (2005) *Maritime Transportation-Safety Management and Risk Analysis*. Elsevier.

Kumar, V. (2007) ‘Optimal contour mapping of groundwater levels using universal kriging — a case study’ , *Hydrological Sciences Journal*, 52(5). doi: 10.1623/hysj.52.5.1038.

Lee, B. (2005) *An Optimal Route Decision and LOS Guidance System for Automatic Navigation of Ships*. Korea Maritime University.

Lee, H. and Kim, C. (2013) ‘An analysis on the relative importance of the risk factors for the marine traffic environment using Analytic Hierarchy Process’ , *Journal of the Korean Society of Marine Environment & Safety*, 19(3), pp. 257–263.

Lee, S., Jeong, Y. and Kim, J. (2014) ‘Clustering Validity Index Based on Support Vector Data Description for Nonhierarchical Clustering’ , *Korean Journal of Business Administration*, 27(12).

Lee, S., Kim, J. and Jeong, Y. (2017) ‘Various Validity Indices for Fuzzy K-means Clustering’ , *Korean Academic Society Of Business Administration*, 46(4).

Lee, S. M. *et al.* (2018) ‘Method for a simultaneous determination of the path and the speed for ship route planning problems’ , *Ocean Engineering*. Elsevier Ltd, 157(April), pp. 301–312. doi: 10.1016/j.oceaneng.2018.03.068.

LG CNS (2018). iSEMS, <http://isems.lgcns.com/LGCNS.ISE.Main/EN/iSEMS/Overview.aspx>. (Accessed 08 Aug 2018).

Li, M. and Liu, Y. (2010) ‘Iso-Map: Energy-efficient contour mapping in wireless sensor networks’ , *IEEE Transactions on Knowledge and Data Engineering*, 22(5), pp. 699–710. doi: 10.1109/TKDE.2009.157.

Li, S. , Meng, Q. and Qu, X. (2012), An Overview of Maritime Waterway Quantitative Risk Assessment Models. *Risk Analysis*, 32: 496–512. doi:10.1111/j.1539-6924.2011.01697.x

Liu, C. and Chen, X. (2014) ‘Vessel track recovery with incomplete AIS data using tensor CANDECOM/PARAFAC decomposition’ , *Journal of Navigation*, 67(1), pp. 83–99. doi: 10.1017/S0373463313000398.

Matheron, G. (1973) ‘The intrinsic random functions and their applications’ , *Advances in Applied Probability*, 5(3), pp. 439–468.

Mazaheri, A. (2009) *Probabilistic Modeling of Ship Grounding*, Helsinki University

of Technology.

Mazaheri, A. *et al.* (2015) ‘Assessing grounding frequency using ship traffic and waterway complexity’ , *Journal of Navigation*, 68(1), pp. 89–106. doi: 10.1017/S0373463314000502.

Ministry of Oceans and Fisheries (2018) Act on the Investigation of and Inquiry into Marine Accidents, Municipal Rule

National Imagery and Mapping Agency (2002) *The American Practical Navigator Originally by Bowditch N. LL. D. Bicentenni.*

Oil Companies International Marine Forum (2016) *Vessel Inspection Questionnaires for Oil Tankers, Combination Carriers, Shuttle Tankers, Chemical Tankers and Gas Tankers. (VIQ 6).*

Park, J.-S, Park, Y.-S. and Na, S.-J. (2008), *Marine Traffic Engineering*, Dasom Publication

Pedersen, P. T. (2010) ‘Review and application of ship collision and grounding analysis procedures’ , *Marine Structures*. Elsevier Ltd, 23(3), pp. 241–262. doi: 10.1016/j.marstruc.2010.05.001.

PIANC (2014) *Harbour Approach Channels Design Guidelines.*

Pietrzykowski, Z. and Uriasz, J. (2009) ‘The ship domain - A criterion of navigational safety assessment in an open sea area’ , *Journal of Navigation*, 62(1), pp. 93–108. doi: 10.1017/S0373463308005018.

Riveiro, M., Pallotta, G. and Vespe, M. (2018) ‘Maritime anomaly detection : A review’ , *WIREs Data Mining and Knowledge Discovery*, 8(5), pp. 1–19. doi: 10.1002/widm.1266.

Rogers, L. W. (2005) *Automating Contour-Based Route Projection for Preliminary Forest Road Designs using GIS.* University of Washington.

Roh, M. Il (2013) ‘Determination of an economical shipping route considering the effects of sea state for lower fuel consumption’ , *International Journal of*

Naval Architecture and Ocean Engineering. Society of Naval Architects of Korea. Production and hosting by ELSEVIER B.V., 5(2), pp. 246–262. doi: 10.3744/JNAOE.2013.5.2.246.

StormGeo (2018) Ship routing services, <http://www.stormgeo.com/solutions/shipping/ship-routing/>. (Accessed 08 Aug 2018).

Swift, A. (1993) *Bridge Team Management*. London.

Szlapczynski, R. (2005) ‘A New Method of Ship Routing on Raster Grids, with Turn Penalties and Collision Avoidance’, *Journal of Navigation*. Cambridge University Press, 59(01), p. 27. doi: 10.1017/S0373463305003528.

Szlapczynski, R. (2011) ‘Evolutionary Sets Of Safe Ship Trajectories: A New Approach To Collision Avoidance’, *Journal of Navigation*. Cambridge University Press, 64(01), pp. 169–181. doi: 10.1017/S0373463310000238.

TIAC (2014) *Marine Inquiry 11-204: Container ship MV Rena grounding on Astrolabe Reef, 5 October 2011, Marine Reports*. Available at: [http://www.taic.org.nz/ReportsandSafetyRecs/MarineReports/tabid/87/ctl/Detail/mid/484/InvNumber/2011-204/Page/19/language/en-US/Default.aspx?SkinSrc=\[G\]skins/taicMarine/skin_marine](http://www.taic.org.nz/ReportsandSafetyRecs/MarineReports/tabid/87/ctl/Detail/mid/484/InvNumber/2011-204/Page/19/language/en-US/Default.aspx?SkinSrc=[G]skins/taicMarine/skin_marine).

Trade Arabia (2018) MHI develops new LNG carrier, http://www.tradearabia.com/news/OGN_270412.html. (Accessed 10 Oct 2018).

Ulusçu, Ö. S. *et al.* (2009) ‘Vessel traffic in the strait of Istanbul’, *Simulation-Based Case Studies in Logistics: Education and Applied Research*, 29(10), pp. 189–207. doi: 10.1007/978-1-84882-187-3_11.

United Nations (2017) *Review of Maritime Transport, 2017*.

Vettor, R. and Guedes Soares, C. (2016) ‘Development of a ship weather routing system’, *Ocean Engineering*. Elsevier, 123, pp. 1–14. doi: 10.1016/j.oceaneng.2016.06.035.

Weathernews (2018) WNI optimum ship routing, <https://global.weathernews.com/your-industry/shipping/>. (Accessed 08 Aug 2018).

- Wikipedia (2018) A*search algorithm,
https://en.wikipedia.org/wiki/A*_search_algorithm (Accessed 06 Dec 2018).
- Yip, T. L. (2008) ‘Port traffic risks – A study of accidents in Hong Kong waters’ , *Transportation Research Part E: Logistics and Transportation Review*, 44(5), pp. 921–931. doi: 10.1016/j.tre.2006.09.002.
- Yoo, B. and Kim, J. (2016) ‘Path optimization for marine vehicles in ocean currents using reinforcement learning’ , *Journal of Marine Science and Technology (Japan)*. Springer Japan, 21(2), pp. 334–343. doi: 10.1007/s00773-015-0355-9.
- Yoo, Y., Choi, H. and Lee, J.. (2015) ‘Comparative Results of Weather Routing Simulation’ , *Journal of the Society of Naval Architects of Korea*, 52(2), pp. 110–118.
- Yoo, S. (2018) ‘Near-miss density map for safe navigation of ships’ , *Ocean Engineering*. Elsevier Ltd, 163(May), pp. 15–21. doi: 10.1016/j.oceaneng.2018.05.065.
- Zhang, D. *et al.* (2017) ‘Enhance the AIS data availability by screening and interpolation’ , *2017 4th International Conference on Transportation Information and Safety, ICTIS 2017 - Proceedings*, pp. 981–986. doi: 10.1109/ICTIS.2017.8047888.
- Zhang, W. *et al.* (2016) ‘An advanced method for detecting possible near miss ship collisions from AIS data’ , *Ocean Engineering*. Elsevier, 124, pp. 141–156. doi: 10.1016/j.oceaneng.2016.07.059.
- Zhen, R., Riveiro, M. and Jin, Y. (2017) ‘A novel analytic framework of real-time multi-vessel collision risk assessment for maritime traffic surveillance’ , *Ocean Engineering*. Elsevier Ltd, 145(September), pp. 492–501. doi: 10.1016/j.oceaneng.2017.09.015.